Physico-chemical of Polyanionic cellulose (PAC-R) polymer on Bonding Ability in the Cementing Material Used for Oil and Gas Well

1. Bekzat Kuvanchbay (ID:201885501)

2. Bektas Tolegen (ID:201714732)

Supervisor: Assoc. Prof. Dr Sonny Irawan

Petroleum Engineering Department

School of Mining and Geosciences

April – 2023

Acknowledgements

We express our deep gratitude to all those who have contributed to the successful completion of this research paper.

Firstly, we would like to thank our principal investigator, Dr. Sonny Irawan for providing us with invaluable guidance and support throughout the research process. His vast knowledge and expertise have been instrumental in shaping our ideas and helping us navigate through the challenges we encountered.

We also extend our heartfelt appreciation to our supervisor Dr Azza Hashim Abbas Babikir, whose constant feedback and constructive criticism helped us refine our research methodology and improve the overall quality of our work. Her patience, dedication, and encouragement have been a great source of inspiration for us.

We are also indebted to the laboratory assistants and research technologists: Yernur Satay, Gylym Sapinov, Madiyar Dyussenkhanov, Farkhad Tarikhov, Gerarldo Davin Aventian who have worked tirelessly with us in collecting and analyzing data. Their diligence and hard work have been instrumental in the success of this research.

We acknowledge the invaluable support we received from all of the above individuals and express our heartfelt gratitude to them.

Statement of originality

This is to confirm that the material of this project is, to the best of our knowledge, our original work. We declare that this project's intellectual substance is entirely our own creation and that all sources used in its preparation have been properly cited.

_____

_____

_____

_____

Abstract

The ability of the cement sheath to bond effectively with the casing or formation depends on its tensile strength and Young's modulus, which determine its ability to withstand deformation under load without separating. The aim of this research was to explore the impact of the concentration of PAC-R copolymer and the duration of curing on the bonding capacity of the cementing substance utilized in oil and gas wells. The study carried out two sets of experiments to assess the chemical and mechanical features of the cement specimens. The compressive strength of the samples was measured after curing for 1 day and 3 days at 80 ℃ in an OFITE curing chamber. The uniaxial test results showed that samples with 10% and 20% PAC-R copolymer concentrations had significantly lower axial loads and axial stresses compared to control samples. As the amount of polymer was raised from 10% to 20%, the compressive strength also went up. This happened because the polymer was able to fill in tiny cracks and gaps in the cement, making the matrix more uniform and compact. As a result, it became more resistant to being compressed. The reduction in the Young modulus was particularly noticeable when using a 10% PAC-R copolymer concentration. As the polymer concentration increased from 10% to 20%, the Young modulus values displayed an inclination to rise.

TABLE OF CONTENTS

CHAPTER-1 INTRODUCTION.....7
1.1. Introduction.....7
1.2. Research Problem.....8
1.2.1. Hypotheses:.....9
1.2.2. Research Questions.....9
1.3. Objectives of the project.....9
1.4. Justification of Research.....10
1.5. Summary.....10
CHAPTER-2 LITERATURE REVIEW.....11
2.1.1. Dimensional and depth data.....12
2.1.2. Wellbore environment, including pressure regime and drilling fluid.....13
2.1.3 Temperature.....14
2.2. Secondary Cementing.....15
2.3. Polyanionic cellulose polymer (PAC-R).....26
2.4. Compressive Strength of cement.....27
CHAPTER-3 METHODOLOGY.....31
3.1. Materials and equipment.....31
3.2. Sample preparation.....33
3.3. Tensile strength measurements.....35
3.4. Microstructure analysis.....36
3.5. Research Flow Chart.....39
CHAPTER-4 RESULTS AND DISCUSSION.....40
4.1. Compressive Strength Analysis.....40
4.2 Flexibility.....42
4.3 FTIR analysis.....43
CHAPTER-5 CONCLUSION AND RECOMMENDATIONS.....47
5.1 Conclusion and recommendations.....47
REFERENCES.....49
Appendix A: Thesis Project Timeline.....53
Appendix B: Project Milestone.....54

List of figures

Figure 1. Three-dimensional survey of a standard vertical well (Nelson and Guillot, 2006)

Figure 2. Cake permeability and dehydration rate of a slurry as a function of the fluid loss additive concentration (after Hook and Ernst, 1969)

Figure 3. Noode buildup after a 45-minute squeeze using slurries with different water loss (after Rike, 1973)

Figure 4. Geometry of perforation (after Binkley, Dumbauld, and Collins, 1958)

Figure 5. Geometry of the cement node (after Binkley, Dumbauld, and Collins, 1958)

Figure 6. Relationship between slurry property, perforation geometry, and height of filter-cake node inside casing (after Binkley, Dumbauld, and Collins, 1958)

Figure 7. Effect of extender on the compressive strength

Figure 8. Effect of antifoam on the compressive strength of cement slurry

Figure 9. OFITE Benchtop Curing Chamber

Figure 10. UCT-1000 Series Unconfined Testing Machine

Figure 11. Nicolet iS10 FTIR Spectrometer

Figure 12. Cement molds

Figure 13. Collect Background interface on OMNIC

Figure 14. Typical Background Spectrum

Figure 15. Research flow chart

Figure 16a. FTIR analysis of sample 1P0

Figure 16b. FTIR analysis of sample 1P10

Figure 16c. FTIR analysis of sample 1P20

Figure 17. FTIR analysis of sample 3P20

Figure 18. FTIR analysis of the EVA polymer by different curing times (after Lanka et al., 2021)

List of Tables

Table1. Cake permeability and dehydration rate of a slurry as a function of the fluid-loss additive concentration (after Hook and Ernst, 1969)

Table 2. Effect of the differential pressure on the permeability of filter cakes and on the filtration rate (experimental) (after Hook and Ernst,l969).

Table 3. Effect of formation permeability on the rate of the filter cake growth (after Hook and Ernst, 1969)
Table 4. Composition of cement slurry
Table 5. Characteristics of samples
Table 6. Results of uniaxial test
Table 7. The comparison of Young Modulus and compressive strength

CHAPTER-1 INTRODUCTION

1.1. Introduction

Primary cementing is the process of placing cement in the annulus between the casing and the formations exposed to the wellbore. The major objective of primary cementing has always been to provide zonal isolation in oil, gas, and water wells, i.e., to exclude fluids such as water or gas in one zone from oil in another zone in the well. To achieve this objective, a hydraulic seal must be created between the casing and cement, also between the cement and the formations, while at the same time preventing fluid channels in the cement sheath. This requirement makes primary cementing the most important operation performed on a well. Without complete isolation in the wellbore, the well may never reach its full producing potential.

Remedial cementing consists of two broad categories: squeeze cementing and plug cementing. Squeeze cementing is the process of placing a cement slurry into the wellbore under sufficient hydraulic pressure to partially dehydrate or expel water from the cement slurry, leaving a competent cement that will harden and seal all voids. Plug cementing is the placement of a limited volume of cement at a specified location inside the wellbore to create a solid seal or plug. Remedial cementing operations are performed for various reasons: to repair faulty primary cementing jobs, alter formation characteristics, repair casing problems, and abandoned wells. Both operations require as much technical, engineering, and operational experience as any primary cement job.

Since the early days, many advances have been made in all of the disciplines associated with cementing. Special Portland cements, manufactured expressly for use in well cementing, allow the industry to use cement systems that are tailored for the conditions encountered downhole. A wide variety of chemical additives makes it possible to place durable cement slurries in wellbore environments ranging from permafrost to geothermal reservoirs. To achieve optimal cement placement and zonal isolation, improved techniques have been developed to condition the wellbore before a primary cement job. Such techniques also reduce the need for remedial cementing. Equipment and techniques have been developed to properly monitor all cement-job parameters. This allows timely decisions during a job to increase the probability of success. Finally, many tools and techniques have been developed to evaluate the quality of the cement job, allowing the operator to make informed decisions regarding future operations. The effect of polymers on mechanical properties of well cement has been actively investigated.

The cementing methods used in Sichuan and Chongqing (2020) have demonstrated that polyanionic cellulose (PAC) and the hydration products of clinker significantly affect cement contamination. PAC is an anionic cellulose ether that has a high degree of polymerization and substitution. It is a commonly used additive in drilling fluids and has a molecular structure that is similar to carboxymethyl cellulose (CMC). However, PAC has superior properties compared to CMC, such as reduced filtration, resistance to salt and collapse, and high-temperature resistance.

It would be of great interest to further explore the bonding ability of PAC-R polymer as an additive in class G cement for oil and gas well cementing. The present work attempts to utilize the unique characteristics of PAC-R polymer, which is one of the most commercial products from construction material with already established production technology, to translate its benefits in oil and gas cementing, which can be further used as additive to enhance bonding ability.

Thus, this work attempts to find the trend of physico-chemical characteristics pertaining to the bonding ability of PAC-R polymer in oilfield cement. In this work, flexibility of the cement system was characterized by Young's modulus and investigated to find the position of PAC-R additive amongst other latex and flexible oilfield cement systems. FTIR spectroscopy was carried out to analyze chemical bonds in PAC-R modified cement systems.

1.2. Research Problem

During hydraulic fracturing, the cement of oil wells experiences a high pressure and alternating stress and may crack due to its hard and brittleness. The cracks could lead to the transmission of formation fluids behind the casing and the formation. A new emerging science on the capillary flow and bonding cement provides solutions to the problem. However, the mechanism of the capillary flow and bonding cement are not well understood. In this work, the Polyanionic cellulose polymer is used as the bonding agent to improve the bonding efficiency in modified cement. The PAC-R-modified cement has excellent repetitive bonding properties compared to other chemicals used, and also withstand High Pressure High Temperature (HPHT). The objectives of this study are 1) to investigate the mechanism of capillary flow and bonding of PAC-R towards pressure, temperature, and PAC-R copolymer concentrations, and 2) to evaluate bonding efficiency of PAC-R-modified cement under high temperature. In this work, the PAC-R polymer is investigated using different methods for evaluating the bonding efficiency such as

bonding strength test and compressive strength test. The microstructure of modified cement is also observed using FTIR. The mechanism of capillary flow and bonding in PAC-R-modified cement with 2 concentrations will be observed towards pressure and temperature applied. Then, the microstructure of the PAC-R-modified cement is investigated to obtain the mechanical and chemical bonding in improving the bonding efficiency. The findings from this study could be useful knowledge in formulating the modified cement mixture using polyanionic cellulose polymer and its optimum concentration to be used in the cement.

1.2.1. Hypotheses:

1. The several PAC-R copolymer concentrations affect the mechanism of capillary flow and bonding that is dependent on temperature and pressure.
2. The physical and chemical bonding play an important role in improving the bonding efficiency.

1.2.2. Research Questions

1. How critical parameters such as concentration, pressure, and temperature are applied affecting the bonding ability in the cement material?
2. How does PAC-R copolymer act as a bonding agent in high temperature conditions?
3. What is the mechanism of capillary flow and bonding in PAC-R co-polymer modified cement?
4. How does the composition of PAC-R co-polymer modified cement help in improving repetitive bonding in the cement material?

1.3. Objectives of the project

The objectives of this project will be as follows:

1. To investigate the trend of physico-chemical characteristics pertaining to bonding ability of PAC-R polymer in oilfield cement.

2. To evaluate bonding efficiency of PAC-R-modified cement by characterizing the compressive strength and young's modulus of the cement system.
3. To analyze chemical bonds in PAC-R modified cement systems using FTIR spectroscopy.

1.4. Justification of Research

The successful outcome of fundamental research will prove the concept and at next the step concept will be used for potential development of PAC-R copolymer as the bonding agent for cement such as to overcome the cracks and micro annulus that are generated by the hydraulic fracturing. In addition, the modified cement will be able to protect the casing string. In which, it will contribute in implementation in Kazakhstan oil and gas fields.

The finding from this experiment could be useful knowledge in formulating the modified cement mixture using PAC-R copolymer and optimum concentration PAC-R copolymer to be used in the cement material.

The capillary flow and bonding mechanism of PAC-R copolymer in this study can be used as a guideline for microstructure study of bonding agents in cement material.

1.5. Summary

The novelties of the project research could be a useful knowledge in formulating the modified cement mixture using PAC-R copolymer and optimum concentration PAC-R copolymer to be used in the cement material. Also, the capillary flow and bonding mechanism of PAC-R copolymer in this study can be used as a guideline for microstructure study of bonding agents in cement material.

This study aims to determine the trend of physio-chemical properties relevant to the bonding ability of PAC-R polymer in oilfield cement. In this study, the tensile strength and Young's modulus were used to define the cement system's flexibility, and the position of PAC-R additive among various latex and flexible oilfield cement systems was investigated. Utilizing FTIR spectroscopy, chemical linkages in an PAC-R-modified cement system were analyzed.

CHAPTER-2 LITERATURE REVIEW

2.1. Primary cementing

Primary cementing is a procedure for injecting cement slurries between the casing and the borehole (Zhang et al. 2022). The main goal of primary cementing has always been to create zonal isolation in oil, gas, and water wells, i.e., to keep fluids as water or gas separate from oil in another zone of the well, since it was first introduced in 1903. In order to accomplish this, a hydraulic seal must be made between the cement and the formations as well as between the cement and the casing, all the while preventing fluid channels in the cement sheath. The most crucial procedure carried out on a well is primary cementing because of this fundamental. The well may never produce to its full capacity if there is no total isolation in the wellbore. Three fundamental forms of well data for the cementing operation must initially be taken into account in order to accomplish its objectives (Nelson and Guillot, 2006).

- Dimensional and depth data
- Wellbore environment, including pressure regime and drilling fluid
- Temperature

The cement characteristics and the displacement regime for a particular well are determined by these facts. Since they limit the density and rheology of the fluids and as a result affect their pump rates, the annular structure and the pore and fracture gradients have a significant impact on the flow regime. The state of the wellbore also reveals whether special materials need to be taken into account because of the presence of gas, salt, or other factors. The selection of additives for regulating the slurry-flow qualities and setting behavior is influenced by these variables, along with the pressure and temperature profiles. The focus of well cementing is to properly install cement in the annulus after a section is drilled as well as to provide zonal isolation between the various zones during the anticipated well life. Any factor that could have an impact on the cement sheath's integrity and the level of isolation both during and after the well's productive life must be carefully taken into account. This is crucial in circumstances where the expense of secondary cementing to fix a poor primary cementing work or restore zonal isolation may be quite costly.

2.1.1. Dimensional and depth data

As noted by Keller et. al. (1983), since depth has a significant impact on temperature, fluid volume, hydrostatic pressure, and dynamic pressure, depth parameters are particularly crucial. High-angle wells provide unique difficulties and need stringent control over mud migration and slurry consistency. Unless directional drilling methods have been proposed, none well is perfectly vertical. A three-dimensional survey of a standard vertical well is demonstrated in Figure 1. The majority of boreholes curve in several ways. If the precise hole trajectory is not available, the somewhat flexible casing string cannot be appropriately centered and may contact the wall of the borehole in various spots (Maeso and Tribe, 2001).

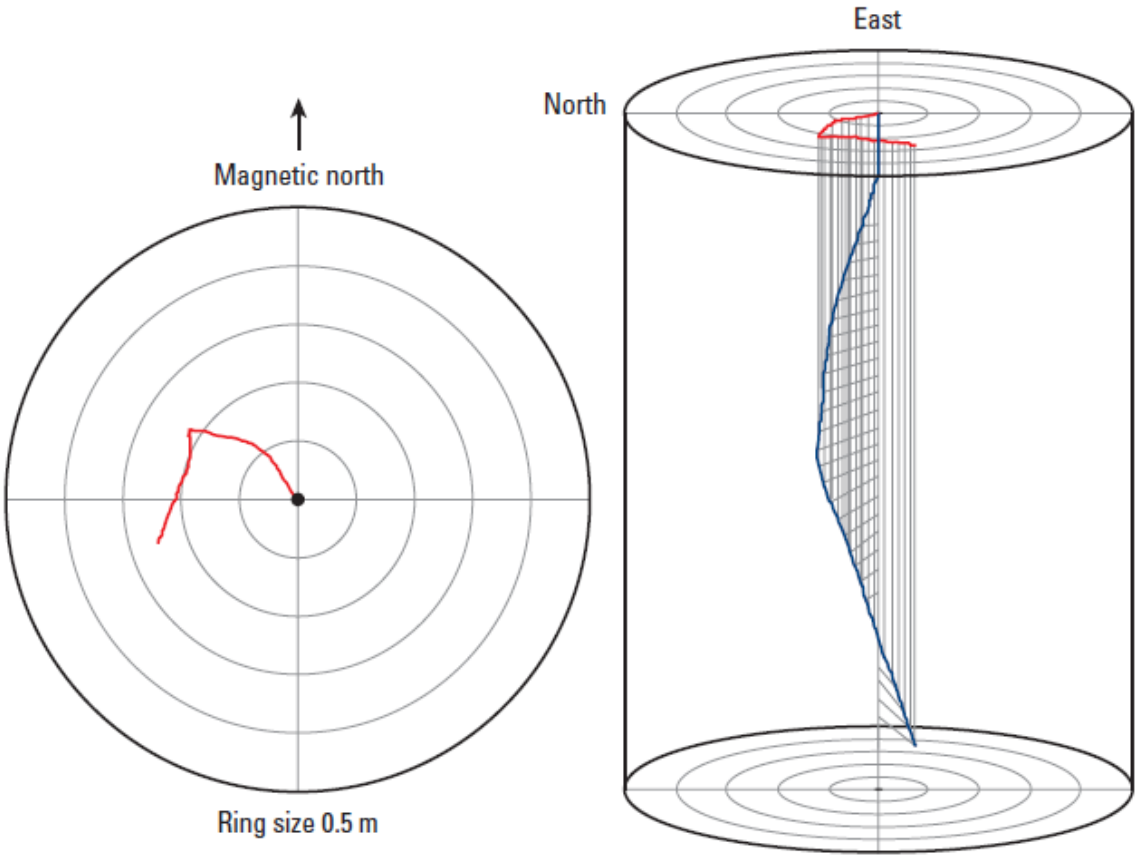

Figure 1. Three-dimensional survey of a standard vertical well (Nelson and Guillot, 2006)

The well path offered adequate information about the correct centralization, mud removal, and zonal isolation, which are obtained by a complete directional survey or

three-dimensional survey of the borehole, which includes measured depth, deviation angle, and azimuth. Otherwise, trajectory uncertainty with a standard deviation value of a few degrees (often 3°) will be used. Also, the differences in trajectory between two survey points using randomized techniques are acceptable. In essence, the open hole size is determined by the size of the drill bit. In addition to the casing size and type, the open hole size must be chosen based on the anticipated well characteristics and completion configuration. Commonly, there is no open hole in a real field with a perfectly round or cylindrical well. Shale-containing formations, poorly consolidated zones are typically unstable. The rock can slough and shatter into particles that are difficult to remove from the wellbore if the formation stresses and mud density are not regulated. The appropriate slurry volume and well control are affected by the variable hole geometry. It has the potential to have a significant impact on displacement mechanics. Diverse wireline caliper instruments have been designed for measuring hole dimensions. Although, in several locations, wireline caliper tools cannot be applied, especially in the huge surface-hole areas. To assure the needed annular fill-up, it is usual practice to specify a certain amount of surplus cement slurry. Such a frequently applied field approach has limitations, as this surplus is mostly reliant on local offset analysis, which takes into account geology, mud, and drilling procedures. Ultrasound may also be used to measure hole size. Due to its great resolution, this method is frequently used to evaluate casing corrosion. With the speed of 140 to 180 times per rotation, the rotating sensor detects the transit time and estimates the standoff. However, the attenuation of the wellbore fluid limits the application of such ultrasonic technology (Nelson and Guillot, 2006).

2.1.2. Wellbore environment, including pressure regime and drilling fluid

The specific issues of the open-hole interval to be cased must be evaluated thoroughly. The existence of pay zones, overpressured formations, low fracture gradients, gas, and extensive salt zones poses difficulties. To tackle these wellbore-related issues, careful task planning is essential. The pressure regime for the whole open-hole area must be considered. Pore pressures are essential for well control, and well logging tools can provide this data. If there are no logging facilities on-site, the mud weight is a reliable indicator of the maximum pore pressure throughout any particular interval. Regardless of whether the mud weight is selected for other factors, as with wellbore stability, it represents the well's pore pressures. When a kick happens while drilling, it offers essential data on pore pressure. The danger probability of fracturing the

formation must be properly considered, and a mean fracture-pressure gradient is often supplied for each open-hole interval. Typically, these values are derived through leakoff testing, which is conducted after the shoe of the preceding casing string has been drilled out, in another case by formation integrity test at any depth of interest. Pay zones require specific consideration. It is essential, for instance, to prevent unwanted damage from cement slurry fluid leakage. Since it does not permeate the formation as extensively as the drilling fluid, the slurry filtrate is typically negligible. When a well is perforated prior to production, the charges usually enter the damaged zone. Cement particles are considerably massive to permeate the matrix of any porous rock. When cementing cracked and/or depleted reservoirs, precautions must be taken to avoid opening cracks and leaking entire slurries deep inside the reservoir. To guarantee optimal long-term well production, productive formations must be adequately insulated from each other and from non producing intervals or reservoirs. When it is confirmed that the formations include gas, specific cement slurries are used in order to prevent gas migration into the column of setting cement (Nelson and Guillot, 2006). As noted by Sauer (1985), cement design is affected by the physical and chemical characteristics of the mud. Cement slurries and drilling fluids are typically inconsistent. Rheological issues and ineffective mud removal have caused the mixing of these fluids. Commonly, chemical washes, spacers, as well as other flush fluids are injected between the drilling fluid and cement slurry to prevent mixing. These fluids are intended to be available to react with both drilling fluid and cement slurry. There is a demand for solvent (surfactants) in spacers or washes to increase compatibility, in order to eliminate the oil layer from the casing and formation contacts, which leads to water getting wet at surfaces (Carter and Evans, 1964). The basic goal of any cementing operation is to completely displace the drilling fluid across the zone of interest. To assist the removal process, the drilling fluid's viscosity should be as low as possible. The predicted downhole parameters of the drilling fluid should be considered since these data may differ considerably from those observed at the surface. It is certainly relevant for OBM because the characteristics of OBM are significantly affected by pressure and temperature (Nelson and Guillot, 2006).

2.1.3 Temperature

The bottom hole circulating temperature (BHCT) and the bottomhole static temperature (BHST) both need to be taken into account, in addition to the difference in temperature between

the bottom and top of the cement column. BHCT is the temperature at which the cement slurry will hypothetically receive as it is inserted in the well. It refers to the temperature applied for high pressure, high temperature (HPHT) thickening time tests of a suggested cement composition. The BHCT prescribes the choice of certain retarders as well as other additives, based upon their efficiency under such particular circumstances. The BHCT is estimated with temperature schedules, which are published in ISO 10426-1:2000 or the regional American National Standards Institute (ANSI)/API 10A/ISO 10426-1-2001 version (published in April 2002). Nevertheless, as proposed by Calvert and Griffin (1998), the ISO/API guidelines do not account for uncommon well circumstances, such as the freezing temperatures encountered in deepwater wells or the high temperatures observed in some deviated wells (Wooley et al., 1984). In addition, they assume that the temperature of surface formation is a constant 80 °F (or 26.7 °C). The API Equivalent Wellbore technique was developed to address these limitations (Kutasov, 2002). This approach recalculates a pseudo length of the wellbore (the equivalent wellbore) and uses a particular equation (the Kutasov-Targhi equation) to obtain the BHCT. The Kutasov-Targhi equation is more effective for deeper wells where the length of the studied segment is minor (negligible) relative to the length of the overall well. The approach does not consider well geometry, flow geometry, or the pumped fluids such as rheology, rate, time, and flow regime for heat exchange. The BHST is the temperature at the bottom of the wellbore that has not been disturbed. BHST is crucial for estimating the rate of compressive strength improvement and the long-term sustainability of a particular cement system. It is often determined using the average geothermal gradient in the region of interest, although data from logging tools may also be used to estimate it. Although ISO/API requirements require compressive strength to be determined at BHST, computer simulations can forecast the pace at which the well temperature will increase from BHCT to BHST (Nelson and Guillot, 2006).

2.2. Secondary Cementing

Secondary cementing or remedial cementing may be described as the process of driving a cement slurry, under pressure, through holes or splits in the casing/wellbore annular area. When the slurry is pressed against a permeable formation, the solid particles filter out on the formation face as the aqueous phase (cement filtrate) enters the formation matrix. A well constructed squeeze job causes the resultant cement filter cake to fill the opening(s) between the formation

and the casing. Upon curing, the cake becomes a virtually impenetrable solid (Suman and Ellis, 1977).

The applications of remedial cementing in both drilling and completion processes is broad. The most important ones are listed below:

- Repair a main cement project that failed as a result of cement bypassing the mud (channeling) or inadequate cement height in the annulus.
- Eliminate water incursion from above, below, or inside the generating zone.
- By separating gas zones from nearby oil intervals, the generating gas/oil ratio (GOR) may be decreased.
- Casing leaks due to rusted or split pipe should be repaired.
- Abandon a zone that is unproductive or depleted.
- To guide the injection into the proper intervals, plug all, a portion, or one or more zones in a multi zone injection well.
- Seal off areas with poor circulation.
- Prevent the movement of fluids into a generating zone.

Regardless of the method used during a squeeze operation, the cement slurry (a suspension of particles) is subjected to differential pressure against a porous rock filter. Filtration is the ensuing physical phenomenon. Filter cake deposition and, in rare instances, formation fracture. Due to the differential pressure, some of the water in the slurry is lost to the porous media. and a cake of cement that has partially dehydrated forms.

The cement cake has a high initial permeability when it forms against a porous layer of sediment (Fig. 2). The cake thickness and hydraulic resistance rise as cement particles build up; as a result, the filtering rate falls and the pressure needed to further dehydrate the cement slurry rises. Four factors influence how quickly filter cakes form:

- permeability of the formation
- differential pressure applied
- Time
- capacity of the slurry to lose fluid at downhole conditions.

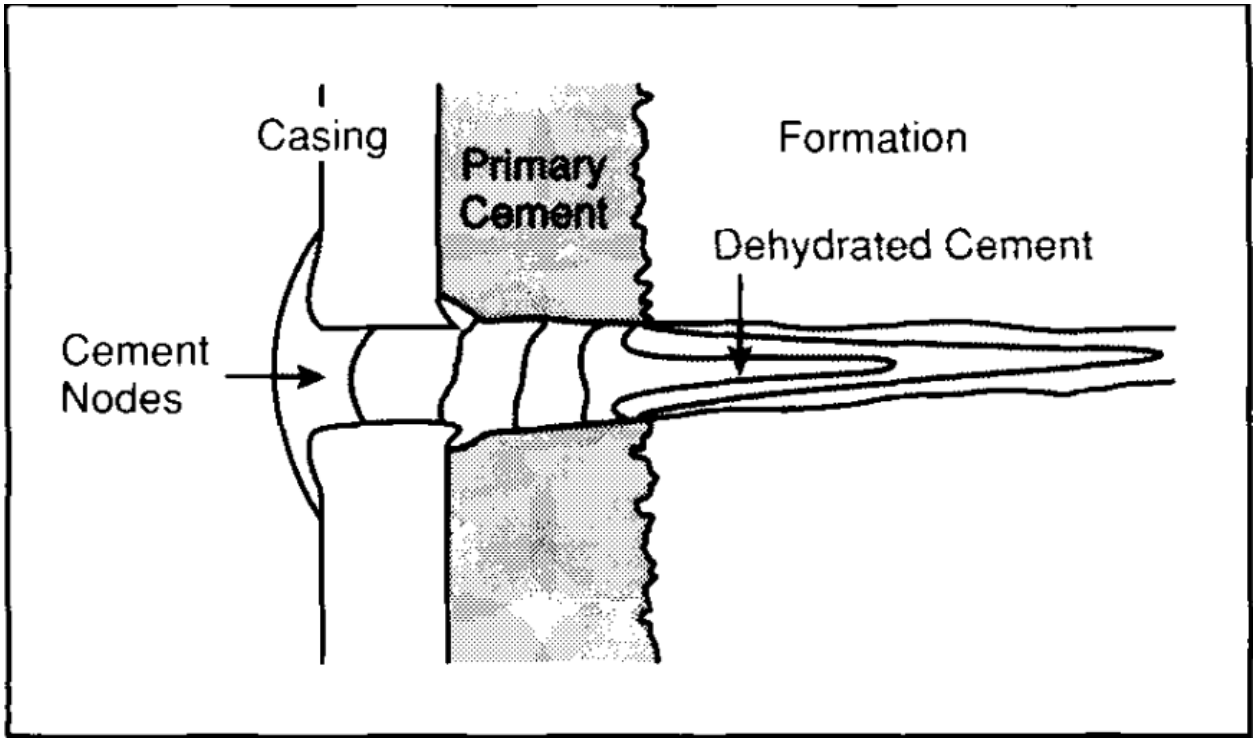

Figure 2. Cake permeability and dehydration rate of a slurry as a function of the fluid loss additive concentration (after Hook and Ernst, 1969)

The rate of fluid loss is closely connected to the rate of slurry dehydration, when it is pressed up against a certain permeability pattern as shown in Fig3. Slurries with low fluid-loss rates dehydrate slowly when pushed against low-permeability formations, and the operation's duration may be too long. Against a formation with significant permeability, a slurry with a high fluid-loss rate dehydrates quickly, as a result, the wellbore may choke with filter cake and channels that would normally receive cement may become blocked. As a result, the optimal squeeze slurry should be designed to regulate the pace of cake growth and enable the homogeneous buildup of a filter cake across all permeable surfaces.

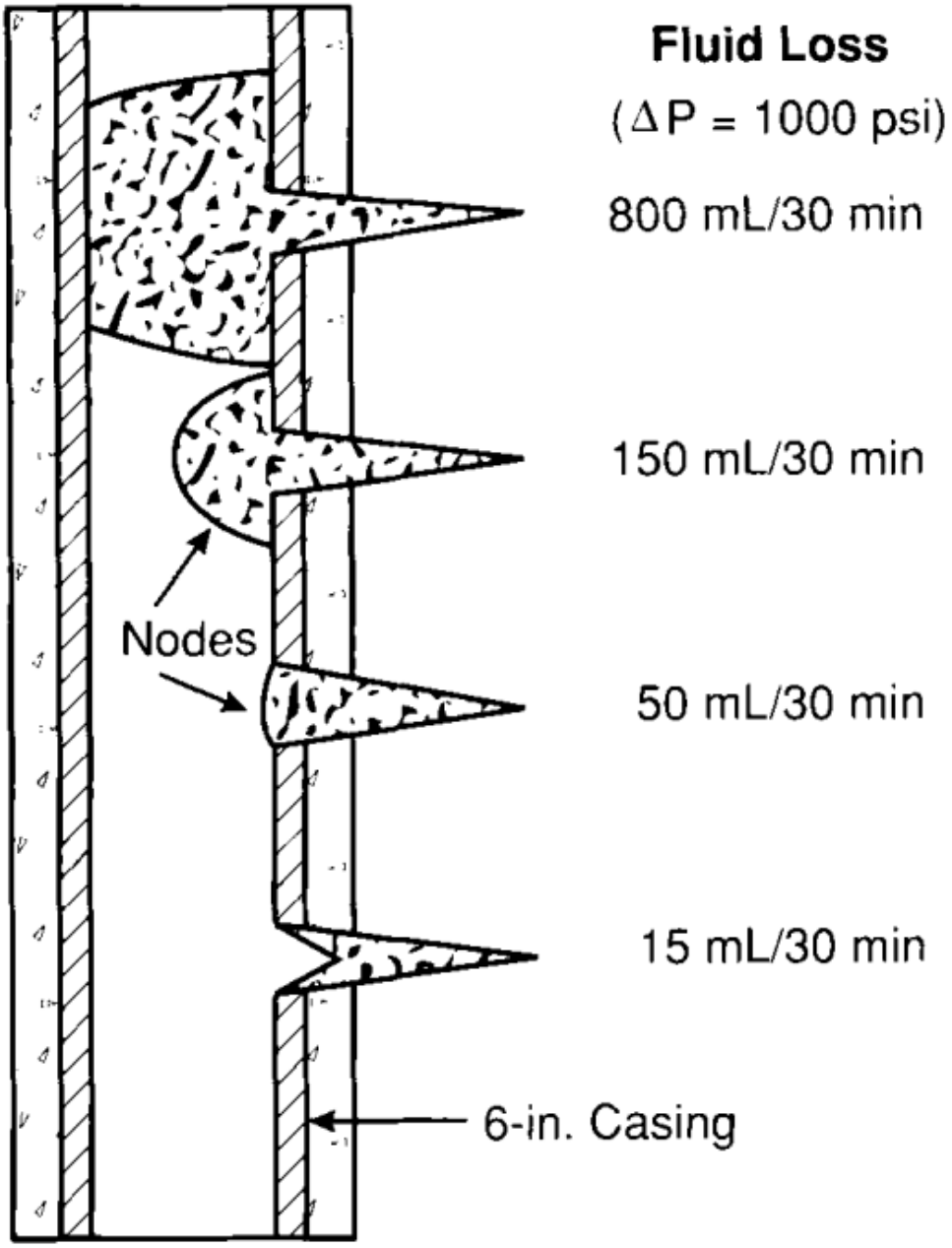

Figure 3. Noode buildup after a 45-minute squeeze using slurries with different water loss (after Rike, 1973)

The basics of theoretical and practical work regarding the fundamentals of' filter-cake deposition in squeeze cementing can be found in the publications of Binkley, Dumbauld. and Collins (1958) and Hook and Ernst (1969).

The law of filter-cake creation for a suspension was created by these authors (such as a cement slurry). A filter cake of thickness dS and porosity is deposited when a volume dQ of filtrate passes through a planar permeable surface of area A. The following set of equations serves as an example of this connection.

$$dS = \frac{f}{1-f-\phi} * \frac{dQ}{A} \quad (2\text{-}1)$$

where f= fraction by volume of solids in the suspension. or

$$f = \frac{V_{solid}}{V_{solid}+V_{liquid}} \quad (2\text{-}2)$$

The ratio $w = f/(1 - f - \phi)$ is called the "deposition constant".

So, the "law of filter-cake formation" can be written as following:

$$\frac{dS}{dt} = wq \quad (2\text{-}3)$$

where

q= flow rate of filtrate per unit area of surface

dS/dt = rate of growth of the filter-cake thickness.

Assuming that the pressure drop across the filtration surface is negligible. Binkley ct al. (1958) applied Darcy's law to the flow of the filtrate through the cake and established the following equations.

1. Growth of a filter cake as a function of filtration time

$$S = \sqrt{\frac{2kw\Delta P}{\mu}} * t^{1/2} \quad (2\text{-}4)$$

where

k = permeability of the filter cake (constant)

μ = viscosity of the filtrate

ΔP = differential pressure

2. Cumulative volume of filtrate as a function of filtration time

$$Q = \sqrt{\frac{2kA^2\Delta P}{\mu w} * t^{1/2}} \quad (2\text{-}5)$$

3. Filter-cake permeability

$$k = \frac{\mu QS}{2At\Delta P} \quad (2\text{-}6)$$

4. Deposition constant

$$W = \frac{AS}{Q} \quad (2\text{-}7)$$

5. Fill up of an unfractured perforation

Binkley et al. (1958) assumed the geometry of perforation as shown in Fig. 4. It is considered that the depth of the perforation is large in relation to its diameter (at least four times). Assuming that the pressure drop in the formation is zero, Binkley et al. (1958) demonstrated that the time required to build a filter cake in close contact with the inside of the casing can be expressed with the following equation.

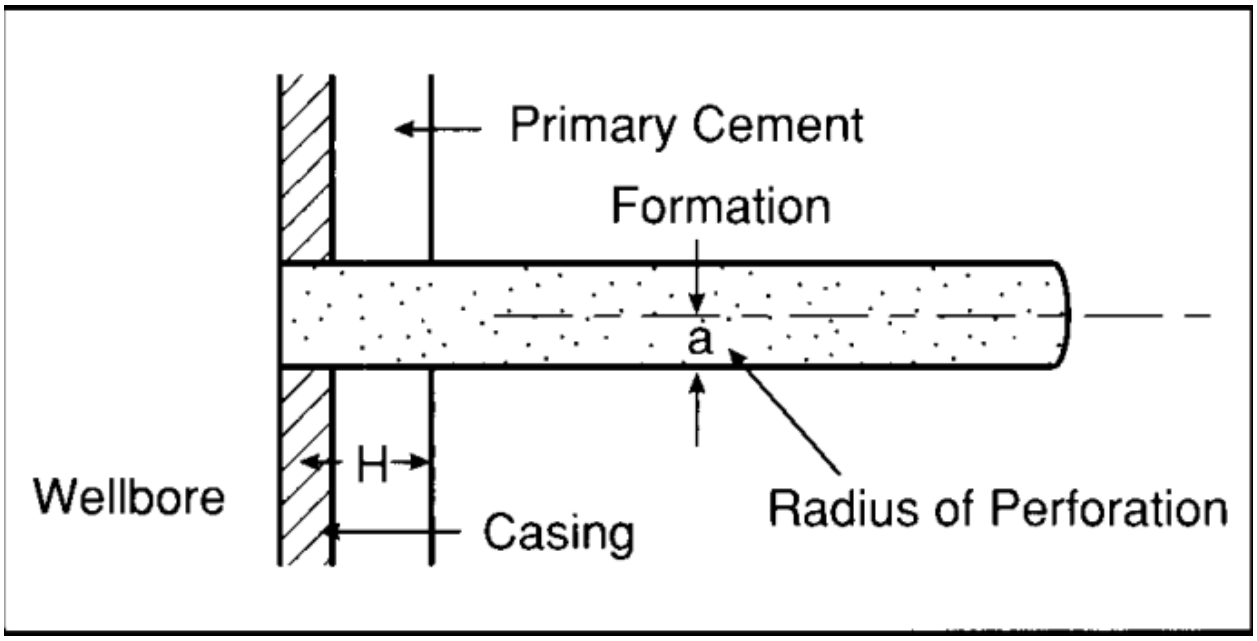

Figure 4. Geometry of perforation (after Binkley, Dumbauld, and Collins, 1958)

$$T = \frac{\mu}{kw\Delta P}\left(\frac{H^2}{2} + \frac{a^2}{4} + e\,aH\right) \quad (2\text{-}8)$$

e was found by experiments to be 0.25. The composition factor, represented by the ratio $\mu/kw\Delta P$, comprises all the elements involved in the cement slurry's deposition characteristics. It's noteworthy to observe that the depth of the perforation has very little influence on the

deposition process when considering the assumption regarding the perforation depth vs. its diameter.

It is possible to calculate the filter-cake permeability k and the deposition constant w by measuring the filter-cake thickness S and the cumulative volume of filtrate Q obtained when a cement slurry comes into contact with a planar permeable surface of area A and is subjected to a differential pressure ΔP for a period of time T.

6. Deposition of solids inside the casing following perforation fill-up

Binkley et al. (1958) assumed that the node forming within the casing has a spherical shape at every stage of development and that the rate of lateral growth is equal to the rate of vertical growth in order to simplify the computation. Fig. 5 provides an illustration of the geometry. The equation below may be calculated if h is the height of the node growing within the casing.

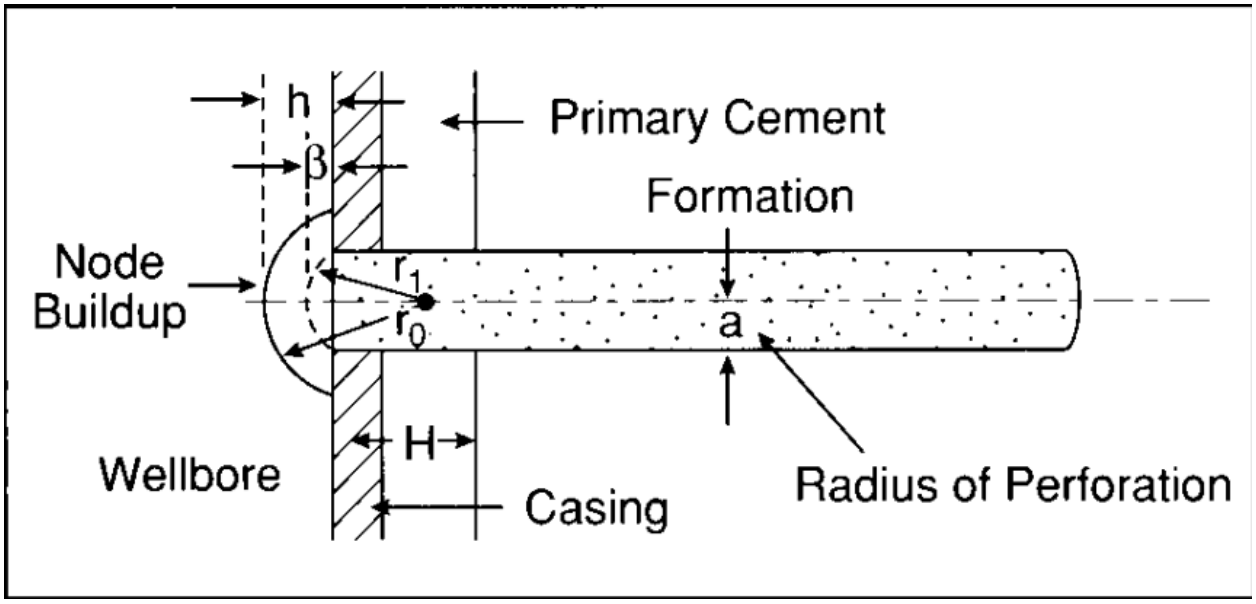

Figure 5. Geometry of the cement node (after Binkley, Dumbauld, and Collins, 1958)

$$\frac{dh}{dt} = \frac{kw\Delta P}{\mu}\left[\frac{1}{(H+\beta+ea)\frac{r_0^2}{r_1^2}+\frac{r_0^2}{r_1^2}-r_0}\right] \quad (2\text{-}9)$$

where

H = combined thickness of the cement sheath and casing,

a = radius of the perforation.

$$\beta = r_1 - \sqrt{r_1^2 - a^2}$$

$$r_0 = \frac{h^2 + (a+h)^2}{2h}$$

$$r_1 = \sqrt{(r_0 - h)^2 + a^2}, \text{ and}$$

$$e = 0.25$$

The results of the numerical integration of this complex equation have been plotted in Fig. 6, which represents the time required to fill a perforation and build a node, vs the ratio Hiu, for different node heights.

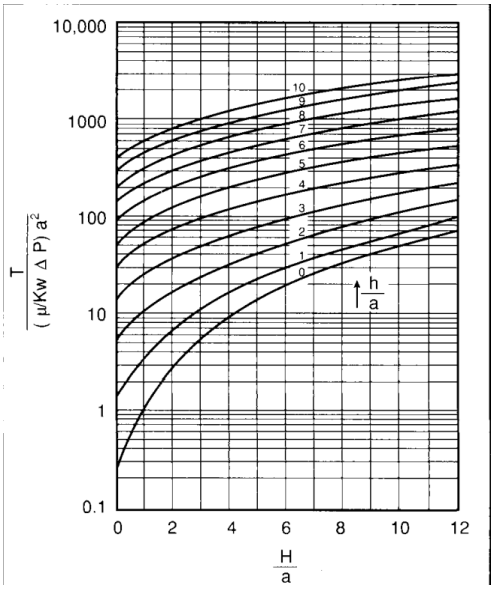

Figure 6. Relationship between slurry property, perforation geometry, and height of filter-cake node inside casing (after Binkley, Dumbauld, and Collins, 1958)

Experimental research was conducted by Hook and Ernst (1969) to determine the effects of formation permeability, differential pressure, and fluid-loss control additives on the rate of filter-cake building. Tables 1, 2, and 3 reveal the results of their analysis.

Table1. Cake permeability and dehydration rate of a slurry as a function of the fluid-loss additive concentration (after Hook and Ernst, 1969)

Slurry - API Class A Cement with Liquid Fluid-Loss Additive and 46% Water			
Concentration of Fluid-Loss Additive (gal/sk)	**API Fluid Loss at 1000 psi (cc/30 min)**	**Permeability of the Filter Cake Formed at 1000 psi (md)**	**Time to Form a 2-in. Thick Filter Cake (min)**
0.00	1200	5.00	0.2
0.07	600	1.60	0.8
0.13	300	0.54	3.4
0.17	150	0.19	14.0
0.19	100	0.09	30.0
0.22	50	0.009	100.0
0.24	25	0.006	300.0

Table 1 contains the results of permeability tests performed on filter cakes made with various amounts of a fluid-loss agent. A neat-cement filter cake's permeability was found to be around 5 MD, which is less than the permeability of many active sandstone formations. The filter cake is about 1,000 times less permeable when the slurry adds enough fluid-loss additive to lower the API fluid-loss rate to 25mL/30 min. This comes close to the permeability of matrix formations, which develop slowly and are challenging to pump through.
Additionally, Table 13-1 demonstrates that the permeability of the filter cake is indirectly related to the rate of filter-cake growth. Fluid-loss additives reduce the filter cake's permeability, which in turn lowers the amount of solids that can be filtered from the slurry.

The information in Table 13-2 shows how squeezing pressure affects the rate of filter-cake development. First, it was established that the permeability of the resultant filter cake is unaffected by changing the squeezing pressure from 500 to 1.000 psi (3.5 to 6.9 MPa). Nevertheless, the results demonstrated that the squeezing pressure had a direct correlation with the pace at which fluid passed through the filter cake, in accordance with Darcy's law.

Table 2. Effect of the differential pressure on the permeability of filter cakes and on the filtration rate (experimental) (after Hook and Ernst,l969).

	Differential of Filter Cake Formation (psi)	**Permeability of the Filter Cake (md)**	**API Fluid Loss at (cc/30 min)**	**Flow Rate Through Filter Cake (cc/min)**
Slurry I	500	5.8	1200	50
	1000	6.0	1200	110
Slurry II	500	1.9	600	17
	1000	1.6	600	30
Slurry III	500	0.53	300	4.7
	1000	0.54	300	9.7

Slurry I - Class A Cement
46% Water

Slurry II - Class A cement
0.5% Dispersant
0.07% gal/sk Liquid Fluid-Loss Additive
46% Water

Slurry III - Class A cement
0.5% Dispersant
0.13% gal/sk Liquid Fluid-Loss Additive
45% Water

The impact of filtration permeability on the rate of cement filter-cake development is shown in Table 3. The time needed to create a filter cake of a given thickness against a 30-md formation is nearly double that seen against a formation with a 300-md permeability. These findings highlight the significance of understanding the formation permeability prior to slurry design.

Table 3. Effect of formation permeability on the rate of the filter cake growth (after Hook and Ernst, 1969)

Time Required for the Formation of a ¼ -in. Long Filter Cake on a 1-in. Diameter Filtration Surface at 1000 psi			
	Bandera Sandstone 30 md	**Berea Sandstone 300 md**	**API 325-mesh Screen**
Slurry I	*6 min*	*2.5 min*	*2.5 min*
Slurry II	*9 min*	*6.5 min*	*6.5 min*
Slurry III	*5 min*	*2.5 min*	*2.5 min*
Slurry I - API Class A Cement 0.5% Dispersant 0.14 gal/sk Liquid Fluid-Loss Additive 46% Water Slurry II - API Class A cement 0.5% Dispersant 0.17% gal/sk Liquid Fluid-Loss Additive 46% Water Slurry III - API Class A cement 0.7% Solid Fluid-Loss Additive 46% Water			

2.3. Polyanionic cellulose polymer (PAC-R)

It is recommended that PAC-R be utilized as a cost-effective solution for reducing the API filtration rate of various water-based drilling fluids. Such fluids may include freshwater, seawater, saturated saltwater, and solids-free brines, in addition to native mud, flocculated mud, inhibited mud, and contaminated systems. PAC-R is capable of increasing and stabilizing the viscosity of these fluids, thereby enhancing their rheology, well hole cleaning, and suspension properties. This is achieved by PAC-R coating and encapsulating cuttings and solids present in the drilling fluids. Moreover, PAC-R is effective across a wide range of pH environments and is known to lubricate solids within the system, improve wallcake characteristics, and reduce the likelihood of experiencing a stuck pipe (John, 2017). Therefore, for effective and efficient drilling operations, PAC-R is recommended as a suitable additive for enhancing the performance of drilling fluids in various water-based systems.

According to studies (Li et al., 2020), the cement slurry will thicken when PAC is added, and this behaviour was particularly pronounced at high temperatures. Cement slurry settles in the area between the wellbore and the casing, causing the casing to sit firmly and steadily in the wellbore, which needs the cement to have a particular compressive strength after curing. The conclusion reached by Zhong (2002) that the polymer additive would increase the flexural strength and toughness of the cement stone but reduce its compressive strength, elastic modulus, and hardness is consistent with the fact that the compressive strength of cured cement rapidly decreases as PAC content increases as shown in Figure 6.

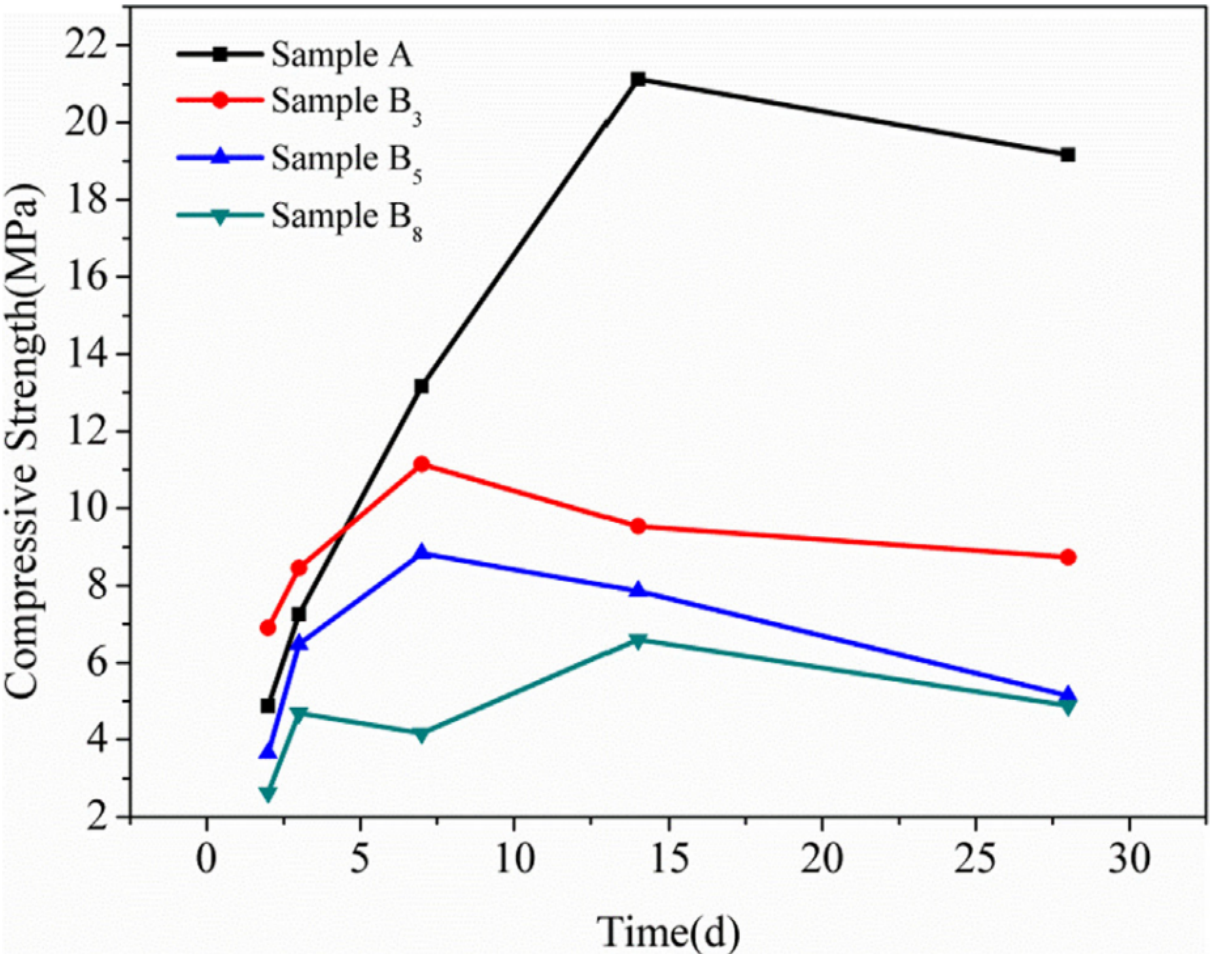

Figure 6. Compressive strength of samples A, B_3, B_5, B_8.

According to Fig. 6, sample B_8's compressive strength is 1/3 of sample A. It is clear from the advanced location of the inflection point that PAC may abbreviate the whole curing time of cement paste and cause partial curing, which may account for the decreased compressive strength. For instance, sample A fully cures in 15 days whereas sample B_3 fully cures in 6 days. The quantity of C-S-H, the primary hydrated product and gel phase in Portland systems that determines the durability and strength of concrete, is likely connected to the amount of PAC that might minimize the hydration products of cement by decreasing the potential curing time.

2.4. Compressive Strength of cement

During drilling operations, cementing is the most significant and costly task. In cementing operations, the annulus between the casing and the nearby rock formation is filled with a specific compound of cement grout and allowed to cure, often over the course of a few

hours or days, to harden and firmly attach the casing to the formation. (Labibzadeh et al., 2010) This compound might be manufactured from a variety of components with varying weight percentages relative to the weight of cement in the grout mixture. The capacity of a material to resist load-induced deformation is one of the qualities used to evaluate the dependability of cementing. The compressive strength of cement concrete is dependent on the kind of raw materials, including additives, mixing proportions, concrete structure, curing process and duration, and environmental factors (Herianto and Fathaddin 2005).

Good compressive strength cement must be able to tolerate abrasive and corrosive forms, a lost circulation zone, carbon (IV) oxide and other poisonous gas intrusions, as well as severe temperatures (Benjamin et al. 2010). Numerous studies using various methodologies have been conducted in this area as a result of issues with inadequate cementing. Sauki and Irawan (2010) investigated the effect of pressure and temperature on well cement degradation by supercritical CO2 and concluded that compressive strength loss was greater at elevated temperature and pressure due to the formation of alpha-calcium silicate, and in the CO2 environment due to the formation of carbonation, which gives the cement temporary strength. Labibzadeh et al. (2010) examined the influence of contemporaneous pressure and temperature fluctuations on the early compressive strength of oil well class G cement and found that a quicker early-age compressive strength might result in a shorter transition phase period (thickening time). Benjamin et al. (2010) also showed that the strength of cement might decrease if crystalline silica was included into the cement slurry.

Numerous experiments were conducted by Zhou and Jia (2010) to produce a low-density, high-compressive strength cement slurry based on the idea of particle grading. The performance of the cement slurry's compressive strength has been enhanced in comparison to the current one. Because of its resistance to high pressure, temperature, and sulphate, class G cement is often employed to seal off formations. Despite these advantages, cement requires additives to increase its properties (Xi et al. 2010). In their research, Bayu et al. (2010) determined that the addition of 0.2% lignosulfonate to a cement slurry enhanced its compressive strength. Above this threshold, it was seen that the compressive strength decreased. The optimum performance of additional additives to boost compressive strength during cement operation is contingent upon the precise concentration of each ingredient. The most effective method is to expose these additions to a series of costly, arduous, and time-consuming experiments (Isehunwa and Orji 1995).

According to Falode et al (2013), using a factorial design, many tests were conducted with the specified slurry systems to determine the compressive strength of class G cement for oil wells. The experiment was done in accordance with API (American Petroleum Institute) specifications (American Petroleum Institute 1997). This study's experiment demonstrated that the compressive strength of cement slurries for certain drilling operations changes depending on the percentage of additives included in their design and formulation. In this study, the effect of different additives on the compressive strength of cement was investigated, and the findings of their sensitivities are shown as clearly in Figures 7 and 8.

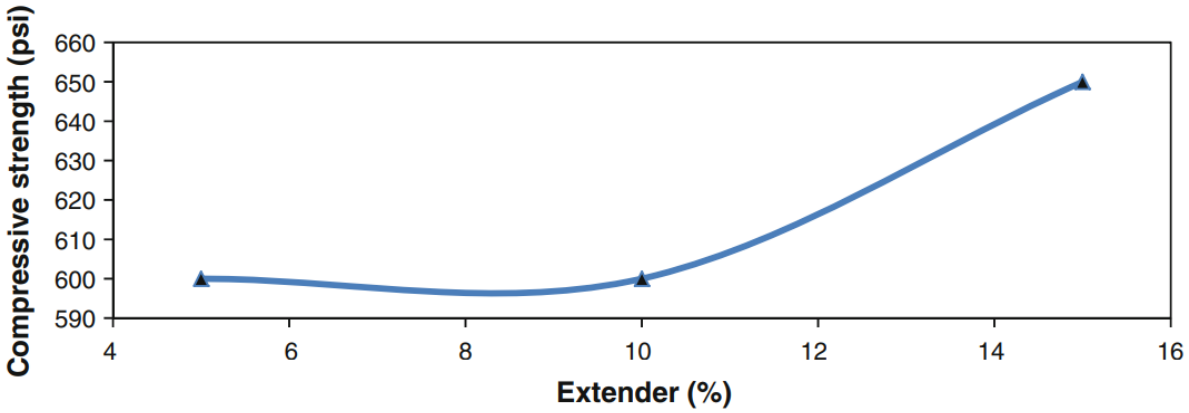

Figure 7. Effect of extender on the compressive strength

It was obvious from Figs. 7 and 8 that both the extender and antifoam had varied effects on the compressive strength of the investigated cement at various proportions and times. This behavior is consistent with the research. At various concentrations, the additives alter the velocity of the acoustic signal with time, hence controlling the amplitude of the Ultrasonic Cement Analyzer's quantifiable response. For instance, the compressive strength of cement stays relatively constant when the extender content increases from 5% to 10%. This pattern continues until 10% extender is added to the slurry; between these intervals, the compressive strength value stays almost constant at 600 psi. However, an increase of 50 psi in compressive strength was seen when the extender was raised from 10% to 15%; this is a result of the growing acoustic signal delay. Figure 7 depicts the impact of the antifoam on the compressive strength of the cement. The threshold value for antifoam inclusion in the cement slurry was around 6%. The compressive strength stays relatively constant at 600 psi below this threshold. Above this amount, the compressive strength continues to decline gradually, and at a proportion of about

8%, a value of 580 psi was measured, reflecting a loss of 20 psi. The design of the slurry must guarantee that the threshold values of these additives are not surpassed in order to keep the compressive strength of the cement, say at 600 psi for a specific application.

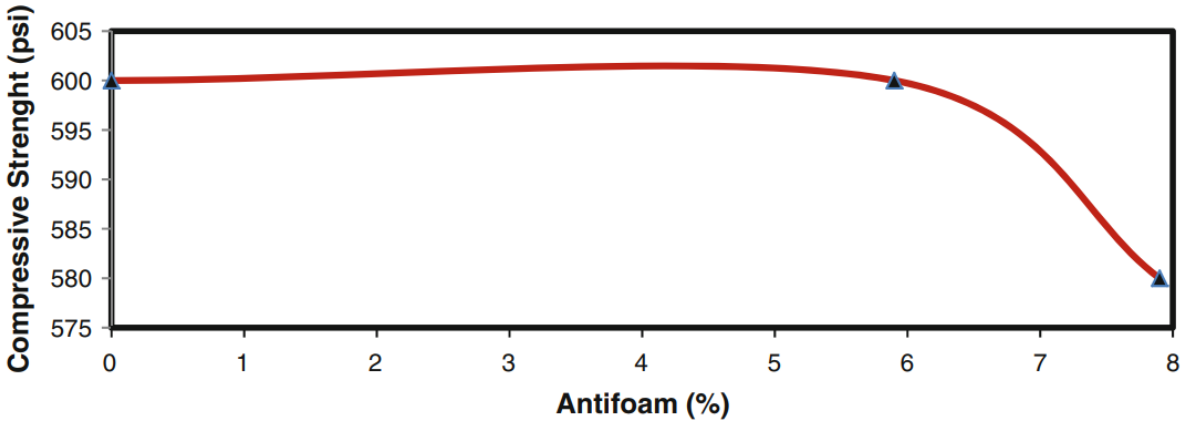

Figure 8. Effect of antifoam on the compressive strength of cement slurry

CHAPTER-3 METHODOLOGY

3.1. Materials and equipment

The materials used for conducting experiments are class API class G oil cement (supplied by NU SEDS laboratory) and Modified Natural Polyanionic Cellulose polymer (PAC-R, supplied by NU SMG laboratory). The equipment used are OFITE Benchtop HTHP Curing Chamber (Provided by NU SMG, 6.407), cement slurry mixer (provided by NU SEDS, 3e.143), UCT-1000 Unconfined Testing Machine (provided by NU SMG, 6.112) and FTIR spectrometer (provided by NU Core Facilities, C4-523).

The OFITE Benchtop curing chamber is used to properly prepare cement specimens for testing on compressive strength. In order for drilling and production to start as soon as feasible, it is vital to ascertain how long it takes for a cement to gain compressive strength. The objective is to create a slurry that can quickly generate compressive strength in order to reduce the amount of time spent "waiting for cement." Cement specimens can be dried in the HTHP Curing Chambers at normal down-hole pressures and temperatures. Chamber's unit may be utilized to test well cements in accordance with API Specification 10. Electronic timer measures elapsed time and may be programmed to terminate test for safety, a pressure relief valve, as well as a safety head with rupture disk are provided.

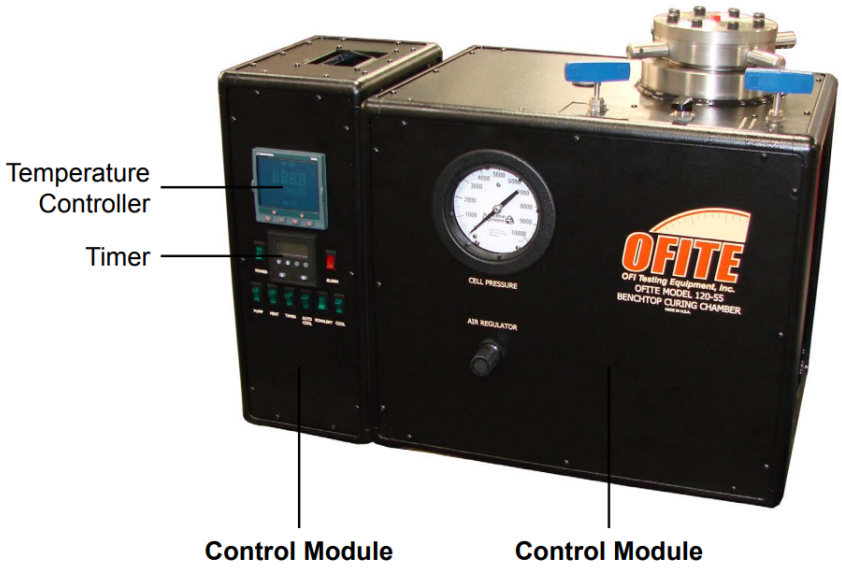

Figure 9. OFITE Benchtop Curing Chamber

UCT-1000 Unconfined testing machine used to determine the unconfined compressive strength of cement samples. The axial actuator is computer-controlled using our state-of-the-art SCON-1400 Wireless Servo Controller and Data Acquisition System and our 64-bit Windows-based software. The system is capable of performing static and dynamic closed-loop tests by controlling the load, deformation, stress, strain or any other measured or calculated parameter. Testing machine has axial load capacity up to 4,500 kN (1,000 kip), axial stroke up to 200 mm, and frame stiffness up to 5,000 kN/mm.

Figure 10. UCT-1000 Series Unconfined Testing Machine

Nicolet iS10 FTIR Spectrometer is used to analyze microstructure of cracked cement samples. The Nicolet iS10 FT-IR spectrometer includes features that validate the instrumental

performance, verify the quality of materials, create SOPs and suitability tests, identify unknowns or mixtures, and quantify mixture ingredients. Spectrometer is equipped with 7800–350 cm^{-1} optimized, mid-infrared KBr beamsplitter and 11000–375 cm^{-1} XT KBr extended range mid-infrared optics.

Figure 11. Nicolet iS10 FTIR Spectrometer

3.2. Sample preparation

All the mixing standards and compressive test techniques comply with API-10 standards (Recommended Practice for Testing Well Cements, 2005) with water to cement ratio of 0.44. The components of cement slurries prepared are provided in Table 1.

Table 4. Composition of cement slurry

Mix	**Designation**	**Cement (g)**	**Water (g)**	**PAC-R Polymer (g)**
Control mix	P0	792±0.5	349±0.5	0
10% Polymer	P10	792±0.5	349±0.5	79.2±0.5
20% Polymer	P20	792±0.5	349±0.5	158.4±0.5

Cement slurry samples were placed in cement molds. The threads of the cell cap were lubricated with high-temperature thread lubricant to prevent stickiness of the cement slurry to the cell walls. Cell caps were placed into the cell and screwed tight. The cap must be tightened consistently and uniformly every time to create a good seal. “Air to cylinder” and ”Pressure release” valves are closed and the pump is switched on. After opening the “Fill cell” valve water will flow into the test cell and the displaced air will be forced out through the loosened thermocouple compression fitting. The temperature of 80℃ was set and the cement slurries were left for 1 day and 3 days.

Figure 12. Cement molds

3.3. Tensile strength measurements.

After curing, the samples were cut in equal cubic parts whose sides were equal to 5 cm. Overall 6 samples were tested for bonding strength. However, a good test was only taken into account when

(i) the fracture started in the center of the disc and

(ii) the crack spread along a vertical line (principal crack) (Labibzadeh, 2010a; Q.Z. Wang and Wu, 2004).

Unconfined testing machine from UCT-1000 series was used, whose loading angle for samples of 50 mm in diameter is ($2\alpha=20°$), and which was kept and shown at the conclusion of each test. Tensile strength and Young's modulus values were determined by averaging at least three measurements from good failure samples. (Q.Z. Wang et al., 2004a) suggested a modified

Griffith criterion for determining tensile strength that takes the loading angle into account and is stated in equation (1):

$$\sigma t = k * \frac{2*P}{\pi*D*t} \quad (1)$$

Where, P = critical load (maximum load during test).

D = diameter of samples (50mm)

t = thickness of samples (50 mm)

k is the coefficient, closely related to loading angle, which is equal to 0.96.

To determine Young's modulus, approximate analytical displacement solutions are typically utilized (Chien and Hung, 2008). Equation (2), modified by (Q.Z. Wang et al., 2004b), which considers the effects of loading angle, was used to get more accurate findings.

$$E = \frac{P}{\pi*\Delta w*t} * \frac{2*\alpha}{sin(\alpha)} * \{(1 - \mu) - ln(1 + \frac{4}{sin(\alpha)^2})\} \quad (2)$$

where E = Young's modulus.

Δw = compression displacement

t = thickness of samples (50mm)

α = loading angle, 10°

μ = Poisson's ratio, 0.3 (Teodoriu et al., 2012).

3.4. Microstructure analysis

Before a sample can be acquired, a background scan must be obtained. Water vapor and carbon dioxide in the air will produce interfering bands which must be subtracted from the spectrum. First we made sure that there is no sample in the beam and the ATR crystal and press are clean. To obtain a background spectrum, Collect – Collect Background was selected as shown below:

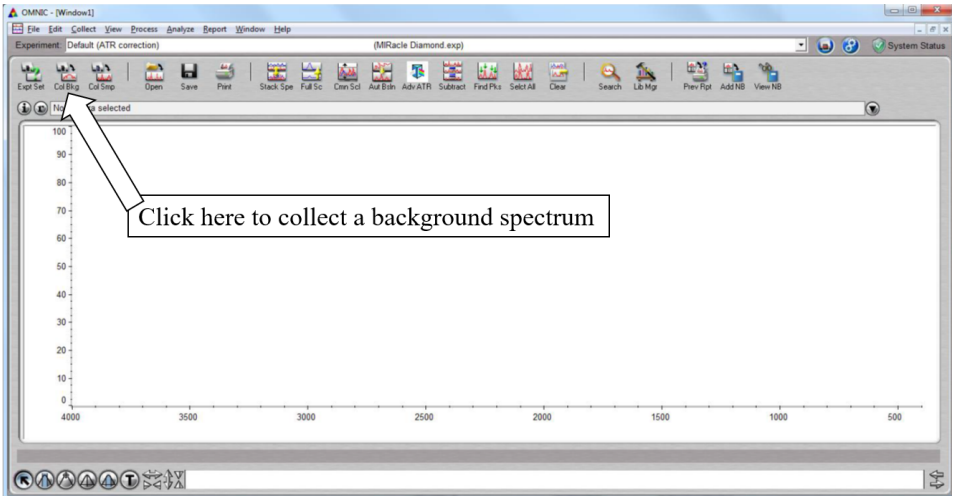

Figure 13. Collect Background interface on OMNIC

The instrument will begin collecting a background spectrum. The bands are observed, which should look similar to that below. If other bands are noted, they may be due to vapor, contamination of the ATR crystal or salt plate if it is previously used. In this case, it is necessary to clean the surface with solvent if needed and observe again. There are often vapors present, particularly if many people have been cleaning the ATR crystal with ethanol, acetone or isopropanol.

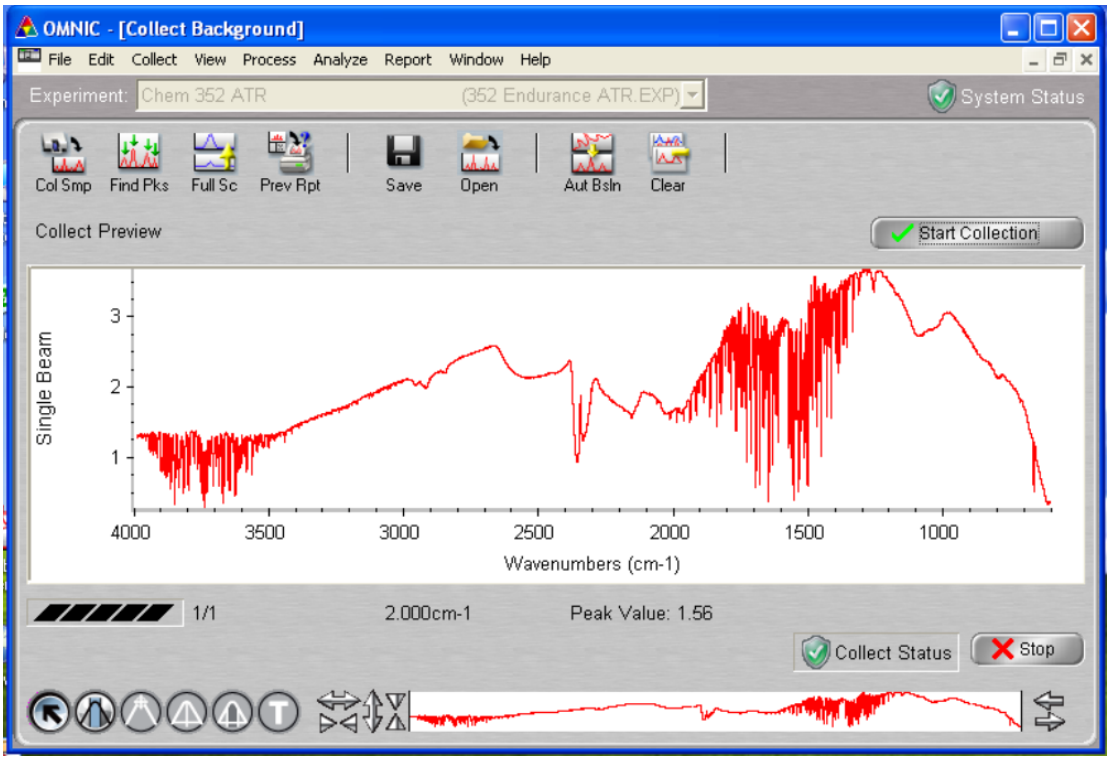

Figure 14. Typical Background Spectrum

Cracked particles from tensile strength tests were used as samples for FTIR analysis. Most samples will be analyzed using the ATR accessory as it is convenient for both liquid and solid samples. Cracked samples were placed in the center of the diamond crystal in the center of the ATR plate. The IR beam is only 0.1 mm in diameter focused on the center of the diamond. OMNIC is a software that operates the FTIR and is used for collecting a sample spectrum. The default units of measurement for FTIR spectra are Transmittance (%) vs Wavenumbers (cm^{-1}). FTIR analysis is done to compare with standard class G cement while examining the microstructure of a novel PAC-R-modified cement before and after exposure to brine and hydrocarbon at various temperatures.

3.5. Research Flow Chart

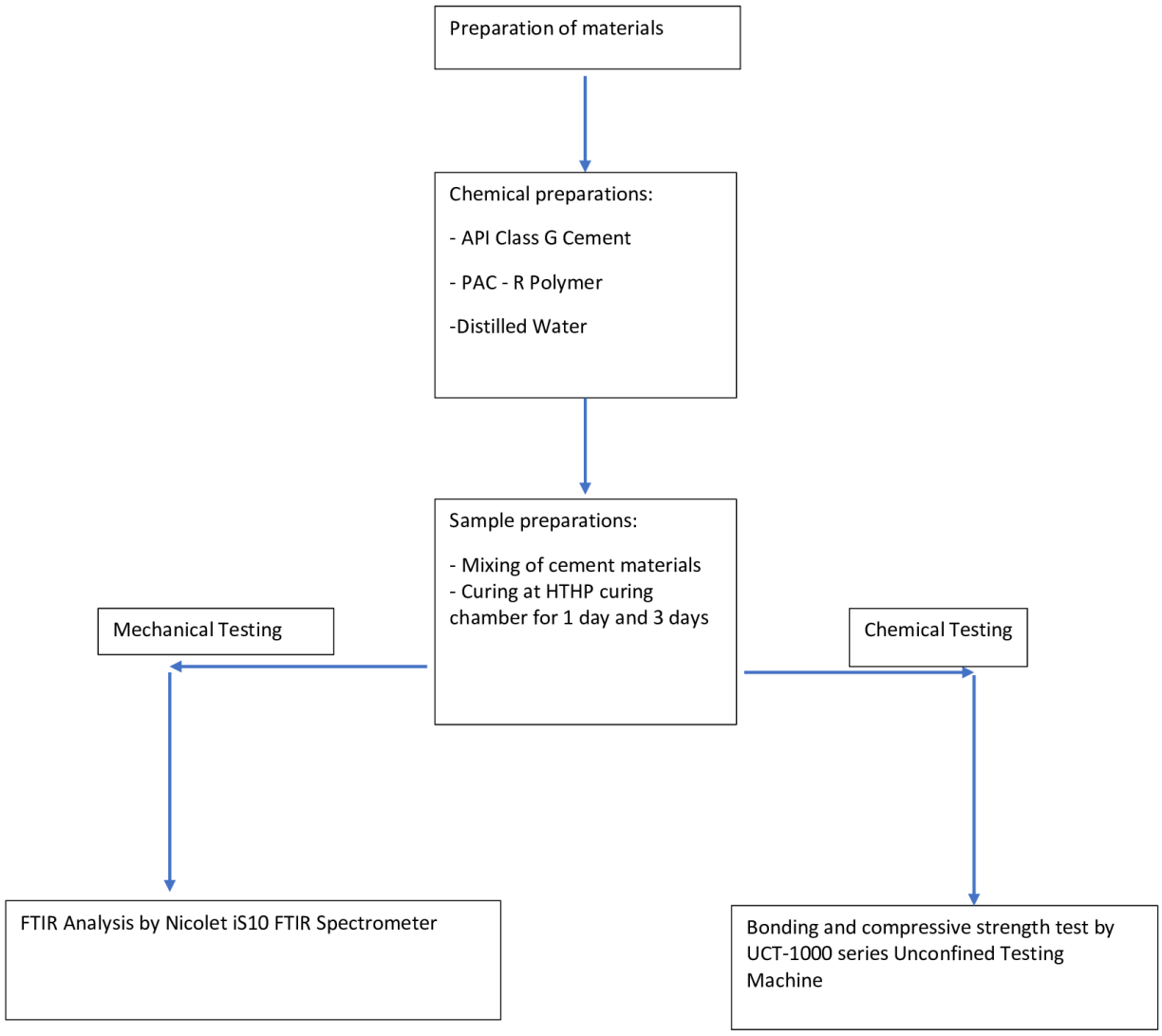

Figure 15. Research flow chart

CHAPTER-4 RESULTS AND DISCUSSION

4.1. Compressive Strength Analysis

In this study, the effect of PAC-R copolymer concentration and curing time on the bonding ability of cementing material used for oil and gas wells were investigated. Two sets of experiments were conducted to evaluate the mechanical and chemical properties of the cement samples.

The curing temperature is an important factor that affects the properties of cementitious materials. In this study, the cement blocks were prepared using an OFITE Curing Chamber at a temperature of 80 degrees Celsius ($176^{\circ}F$). This temperature was chosen based on previous studies of Yao and Hua (2007) and Sun et al. (2006) that have shown that higher curing temperatures can accelerate the hydration process and improve the strength of cementitious materials. The use of a curing chamber also ensures that the samples are cured in a controlled environment, which helps to minimize the effects of external factors such as temperature change and humidity.

Table 5. Characteristics of samples

Designation	Curing time (days)	Polymer Concentration (%)
1P0	1	0
1P10	1	10
1P20	1	20
3P0	3	0
3P10	3	10
3P20	3	20

Note: 1P0 - 1 day of curing with 0% BWOC, 1P10 - 1 day of curing with 10% BWOC, 1P20 - 1 day of curing with 20% BWOC, 3P0 - 3 days of curing with 0% BWOC, 3P10 - 3 days of curing with 10% BWOC, 3P20 - 3 days of curing with 20% BWOC,

The mechanical properties of six cement blocks with varying concentrations of PAC-R copolymer and curing times were analyzed and presented in Table 5. Designation 1P0 is defined as 1 day of curing time at 0% BWOC as well as 3P10 3 days of curing time at 10% BWOC.

Samples 1P0 and 3P0 were used as control mixes without any PAC-R copolymer. From the uniaxial test, the values of axial loads of samples were obtained. These values indicate the maximum axial load for each sample before the failure. The axial stresses were calculated by the ratio of axial loads to the cross-sectional area of the cement blocks during the uniaxial test, which is also defined as compressive strength. Compressive strength values illustrate the same trend as the values of axial load. The results of the uniaxial test showed in Table 6 where samples with 10% and 20% PAC-R copolymer concentrations had significantly lower axial loads and axial stresses compared to control samples, the similar tendency was observed in the studies of Sun et al. (2006), Wang and Wang (2011), Yang et al. (2015) and Richhariya et al. (2020). In the research of Wang and Wang (2011) and Yang et al. (2015), Ethylene-Vinyl Acetate (EVA) copolymer additive has demonstrated gradual reduction of the compressive strength by increasing the polymer quantity in the cement slurry content. The similar results were obtained with Styrene Butadiene Latex (SBL) and Dual Coated Polyacrylamide (DPAM) (Yang et al., 2015; Richhariya et al., 2020). The reduction in the compressive strength is ascribed to the existence of organic constituents within the matrix (Lanka et al., 2021). However, as the polymer content was increased from 10% to 20%, there was a subsequent increase in compressive strength. This can be attributed to the ability of the polymer to fill in micro-cracks and voids in the cement matrix, resulting in a more homogeneous and denser matrix that can resist compressive forces better. Additionally, some polymers may also have adhesive properties that enhance bonding between cement particles, contributing to increased strength (Carballosa et al.). Potentially, it may be referred to the PAC-R copolymer.

Additionally, increasing the curing time from 1 day to 3 days resulted in a significant increase in the axial load and axial stress of the cement blocks, regardless of the PAC-R copolymer concentration. The compressive strength of cement increases with increasing curing time, as the hydration reaction between cement particles and water continues to form more cementitious products and results in denser and stronger cement matrix (Raheem, 2013).

Table 6. Results of uniaxial test

Designation	Axial Load (kN)	Compressive strength (kPa)
1P0	74.3	29720
1P10	0.5	200
1P20	0.7	280
3P0	124.2	49674.8
3P10	1.6	636.5
3P20	6.8	2720

4.2 Flexibility

The study by Lanka et al. (2021) has demonstrated the flexibility of G class cement through a reduction in elastic modulus. The Young modulus values were also computed for each sample, revealing that the addition of PAC-R copolymer to the cementing material resulted in a decrease in the Young modulus of the cement blocks (Table 7). This decrease in the Young modulus was more pronounced with a 10% concentration of PAC-R copolymer, as the Young modulus values exhibited a trend of increasing with an increase in polymer concentration from 10% to 20%. However, the elastic modulus growth from 1P10 to 1P20 was deemed insignificant, remaining at almost the same value. In contrast, an increase in curing time from 1 day to 3 days led to a significant increase in the Young modulus of the cement blocks, irrespective of the PAC-R copolymer concentration.

Table 7. The comparison of Young Modulus and compressive strength

Designation	Compressive Strength (kPa)	Young Modulus (MPa)
1P0	29720	1486
1P10	200.00	2.725
1P20	280.00	5.091
3P0	49675	3161
3P10	636.54	8.416
3P20	2720.0	21.76

Similar observations were reported by Thiercelin et al. (2018), who studied the flexibility of class G cement by examining the decline in elastic modulus with the addition of latex and an increase in curing time. Their research revealed that the elastic modulus value with latex additive, under curing conditions of 3 days, $80^{\circ}C$, and 3000 psi, was 4.07 GPa. This value exhibits a significant difference from the values obtained from Table 7. The lower values obtained from the test results of the PAC-R cement under investigation may be attributed to dissimilar curing conditions and the absence of pressure during the lower curing time compared to the rest of the cement system. This difference in curing conditions may explain the smaller values obtained when compared to the latex cement. However, in cementing oil and gas wells, very low values of Young modulus may indicate inadequate strength and stiffness of the cement, potentially leading to cement failure and reduced zonal isolation.

4.3 FTIR analysis

The chemical properties of the cement samples using Fourier transform infrared spectroscopy (FTIR) were analyzed. The FTIR results showed that the addition of PAC-R copolymer to the cementing material led to the formation of new chemical bonds between the PAC-R copolymer and the cement particles.

FTIR graphs of neat cement, 10% BWOC (by weight of cement), 20% BWOC without

changes in curing time are illustrated in the Fig. 16a, Fig 16b, Fig16c. In these figures the numbers 1, 2, 3 illustrate the peaks.

Peak 1 ($2950\ cm^{-1}$) in the FTIR spectrum of cement or PAC-R additive with cement corresponds to the stretching vibration of the -CH3 and -CH2 functional groups in the aliphatic hydrocarbons. This peak is commonly observed in organic compounds, including polymers, and can also be present in cement or cement additives that contain organic components. In the case of PAC-R additive with cement, the peak at $2950\ cm^{-1}$ may be influenced by the presence of the organic polymer. PAC-R is a water-soluble polymer that is derived from cellulose and contains aliphatic hydrocarbon chains. The presence of the PAC-R additive in the cement can contribute to the intensity of the peak at $2950\ cm^{-1}$ in the FTIR spectrum. Therefore, the peak at $2950\ cm^{-1}$ in the FTIR spectrum of cement or PAC-R additive with cement is an indication of the presence of aliphatic hydrocarbons, which may be derived from organic components in the sample or the PAC-R additive. This peak can provide information on the organic content of the cement or the influence of organic additives on the cement.

Peak 2 ($2350\ cm^{-1}$) in the FTIR spectrum of cement or PAC-R additive with cement corresponds to the stretching vibration of the triple bond of carbon dioxide (CO2). This peak is usually observed when the sample is exposed to air, as CO2 in the atmosphere can react with the free calcium hydroxide (Ca(OH)2) in the cement to form calcium carbonate (CaCO3) through carbonation. The formation of CaCO3 is a slow process and can take several days or even weeks to occur, depending on the environmental conditions. Therefore, the peak at $2350\ cm^{-1}$ in the FTIR spectrum of cement or PAC-R additive with cement is an indication of the carbonation of the sample and the presence of CaCO3. The intensity of this peak can be used to monitor the degree of carbonation of the sample and to assess the performance of the cement or the PAC-R additive under different environmental conditions. The decrease in transmittance at peak 2 from neat cement to the cement with PAC-R additive indicates that the sample is absorbing more infrared radiation at that wavenumber, which can be attributed to the presence of CaCO3 chemical bonds.

Peak 3 ($1080\ cm^{-1}$) in the FTIR spectrum of cement or PAC-R additive with cement corresponds to the stretching vibration of the Si-O-Si bond in the silicate minerals present in the cement. This peak is commonly observed in the FTIR spectrum of cement and is used to identify

the presence of various silicate minerals, such as aluminosilicates and calcium silicates, which are the main components of cement. In the case of PAC-R additive with cement, the peak at $1080\ cm^{-1}$ may be influenced by the presence of the additive. The PAC-R additive may interact with the silicate minerals in the cement and affect the vibrational energy of the Si-O-Si bond, which could result in changes in the peak position or intensity at $1080\ cm^{-1}$ (Fig.16b and Fig.16c) in the FTIR spectrum.

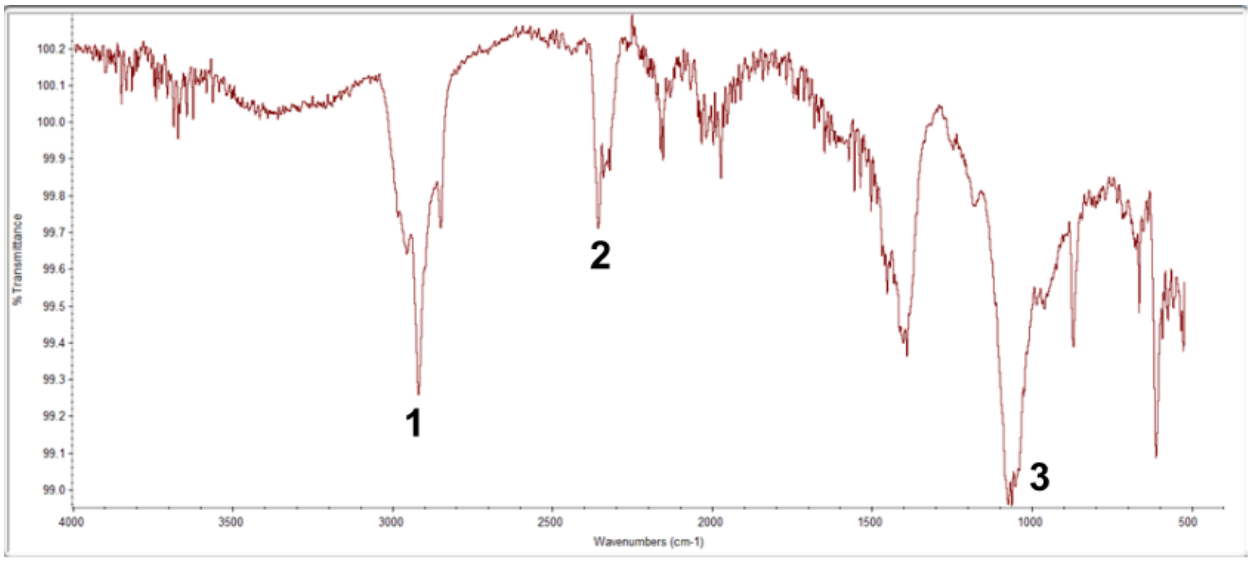

Figure 16a. FTIR analysis of sample 1P0

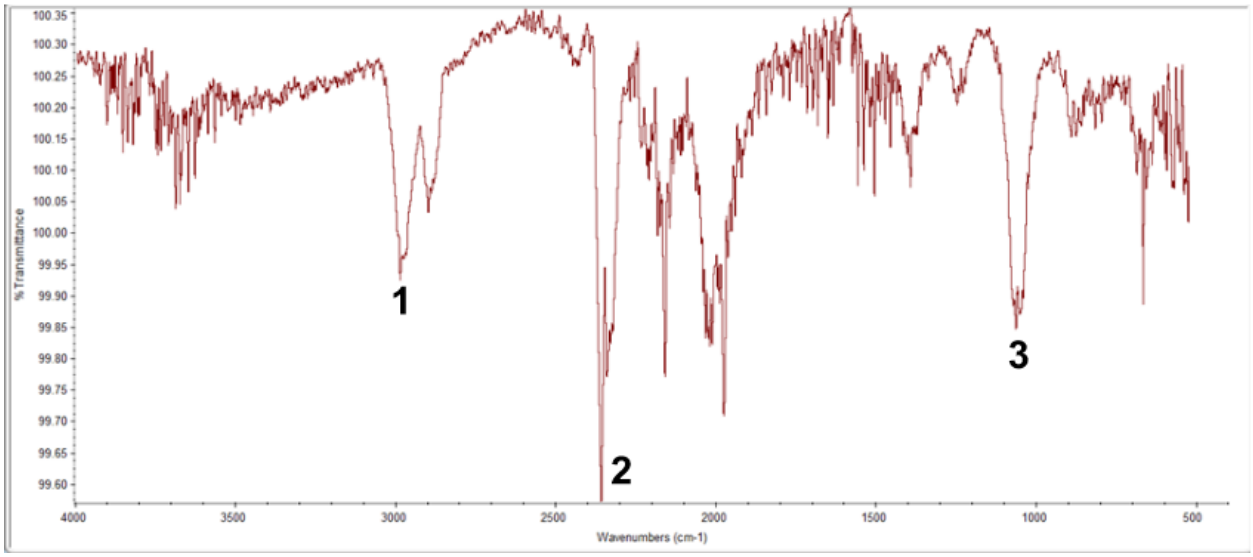

Figure 16b. FTIR analysis of sample 1P10

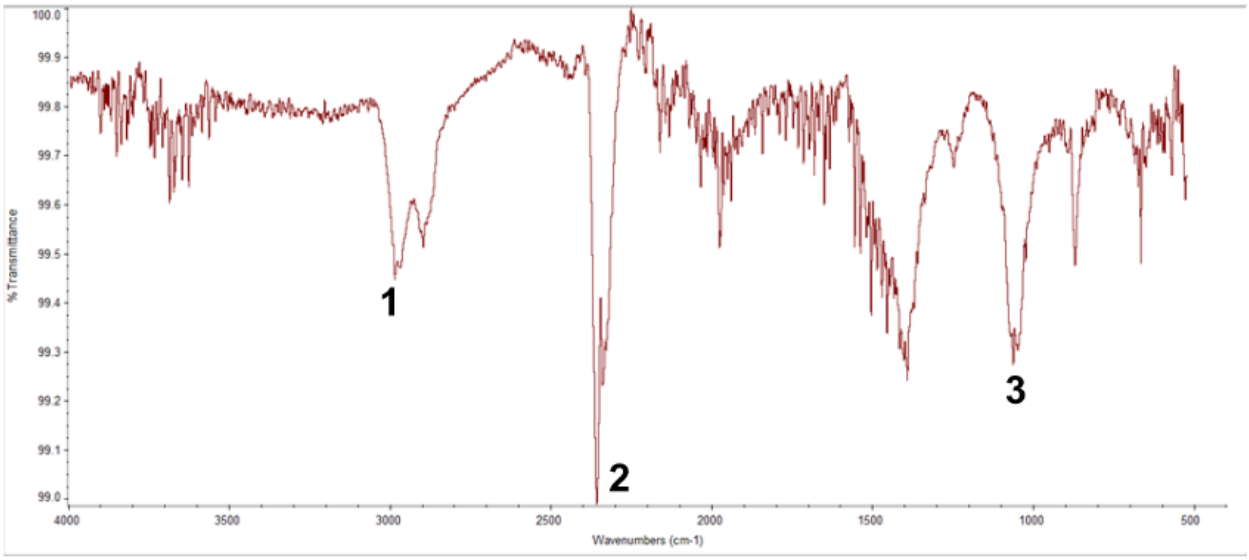

Figure 16c. FTIR analysis of sample 1P20

The samples in Fig.16 c and Fig.17 have the equal distribution of PAC-R concentration in the content with different curing times. There is a tendency at peak 3, where at similar wavenumbers the absorbance has increased. It is an indication of increasing Si-O-Si bonds from the functional group due to the extension of curing time. The analogous tendency has been observed in the studies of Lanka et al. (2021) with the extension of curing time between the equivalent EVA copolymer concentration (Fig. 18).

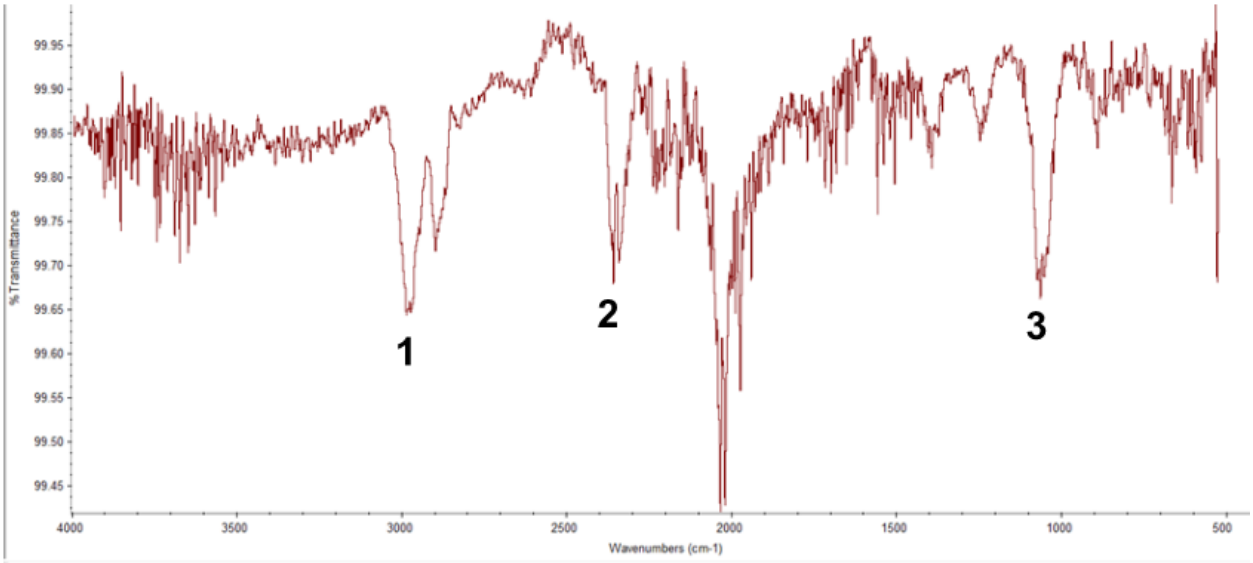

Figure 17. FTIR analysis of sample 3P20

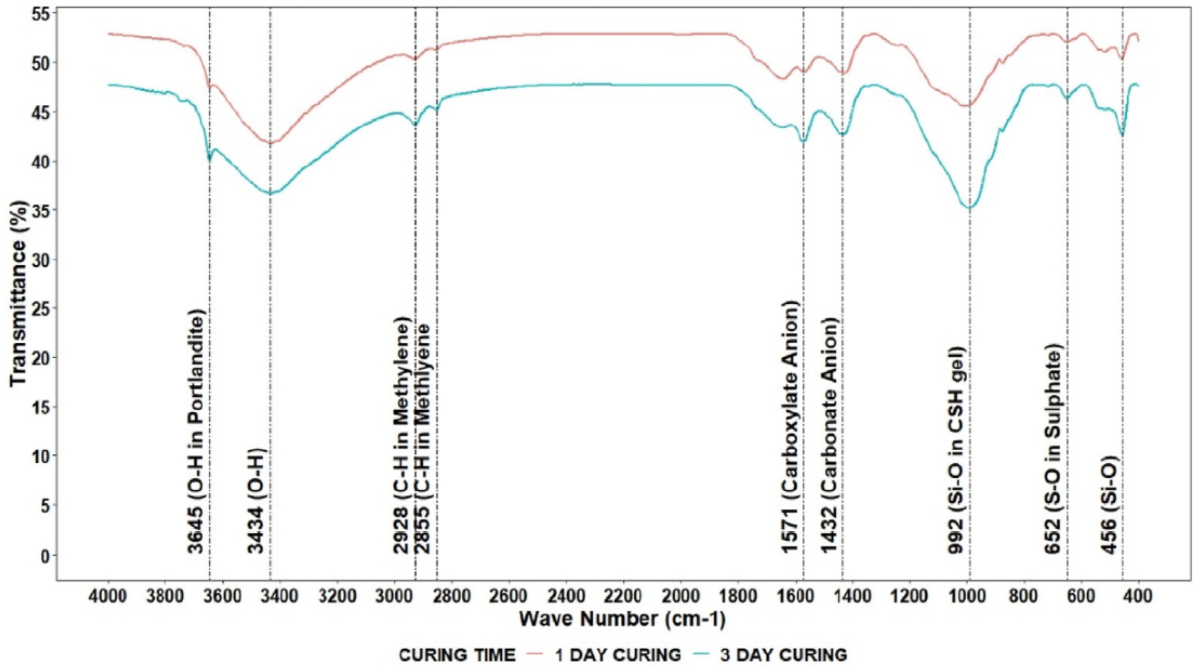

Figure 18. FTIR analysis of the EVA polymer by different curing times (after Lanka et al., 2021)

CHAPTER-5 CONCLUSION AND RECOMMENDATIONS

5.1 Conclusion and recommendations

In this research paper, the physico-chemical characteristics of Polyanionic cellulose (PAC-R) polymer were investigated to determine its effect on the bonding ability of oilfield cement. The objectives of the study were achieved, and the results indicated that the addition of PAC-R copolymer to the cement system had both positive and negative effects on its bonding efficiency.

The further recommendation for this study is connected to the curing process. There is a dissimilar curing technique with varying pressure conditions. The usage of pressure leads to the HPHT condition. presumably, the absence of pressure affects the lower values of strength and elastic modulus.

The study revealed that the addition of PAC-R copolymer to the cement system led to a decrease in the Young modulus of the cement blocks. This decrease was more pronounced with a 10% concentration of PAC-R copolymer, while the elastic modulus growth from 1P10 to 1P20 was deemed insignificant, remaining at almost the same value. Additionally, an increase in

curing time from 1 day to 3 days led to a significant increase in the Young modulus of the cement blocks, regardless of the PAC-R copolymer concentration.

The compressive strength values follow the same pattern as the axial load values. The results of the uniaxial test revealed that the samples with 10% and 20% PAC-R copolymer concentrations experienced lower axial loads and axial stresses compared to the control samples. However, the compressive strength increased with an increase in polymer content from 10% to 20%. This may be because the polymer can fill the micro-cracks and gaps in the cement matrix, which results in a more uniform and compact matrix that can resist compressive forces better. Furthermore, certain polymers may also have an adhesive quality that improves the bond between cement particles, resulting in increased strength.

Furthermore, the FTIR spectroscopy analysis revealed that the chemical bonds in the PAC-R modified cement system were similar to those in the neat cement system. This suggests that the PAC-R copolymer does not interfere with the chemical bonding in the cement system.

Based on the findings of this study, it can be concluded that PAC-R polymer is not recommended for use in oil well cementing due to the decrease in Young modulus values. This decrease in the Young modulus may indicate inadequate strength and stiffness of the cement, potentially leading to cement failure and reduced zonal isolation. Therefore, further research should focus on developing alternative materials that can improve the bonding ability of oilfield cement without compromising its mechanical properties.

In conclusion, this study provides valuable insights into the effects of PAC-R polymer on the bonding ability of oilfield cement. The findings of this study can serve as a basis for further research in this field and contribute to the development of new materials for oil and gas well cementing.

REFERENCES

Benjamin, I., Joe, M. and Daniel, B., 2010. Strength retrogression in cements under high-temperature conditions. In *35th Workshop on Geothermal Reservoir Engineering, Stanford University, Stanford, California*.

Betioli, A.M., Gleize, P.J.P., John, V.M. and Pileggi, R.G., 2012. Effect of EVA on the fresh properties of cement paste. *Cement and Concrete Composites*, *34*(2), pp.255-260.

Binley, G.W., Dumbauld, G.K. and Collins, R.E., 1958. Factors affecting the rate of deposition of cement in unfractured perforations during squeeze-cementing operations. *Transactions of the AIME*, *213*(01), pp.51-58.

Calvert, D.G. and Griffin, T.J., 1998, March. Determination of temperatures for cementing in wells drilled in deep water. In *IADC/SPE drilling conference*. OnePetro.

Carballosa, P., Calvo, J.G., Revuelta, D., Sánchez, J.J. and Gutiérrez, J.P., 2015. Influence of cement and expansive additive types in the performance of self-stressing and self-compacting concretes for structural elements. *Construction and Building Materials*, *93*, pp.223-229.

Carter, L.G. and Evans, G.W., 1964. A study of cement-pipe bonding. *Journal of Petroleum Technology*, *16*(02), pp.157-160.

Chien, C. Ma, Hung. K.M., 2008. Exact full-field analysis of strain and displacement for circular disks subjected to partially distributed compressions. Int J. Mech. Sci, 50 (2), 275-292. https://doi.org/10.1016/j.ijmecsci.2007.06.005

Herianto A, Fathaddin MT (2005) Effects of additives and conditioning time on comprehensive and shear bond strengths of geothermal well cement. In: Proceedings of world geothermal congress. Antalya, Turkey, pp 1–7

Hook, F.E. and Ernst, E.A., 1969, May. The Effect of Low-Water-Loss Additives, Squeeze Pressure, and Formation Permeability on the Dehydration Rate of a Squeeze Cementing Slurry. In *SPE Rocky Mountain Regional Meeting*. OnePetro.

Isehunwa, S.O. and Orji, H.I., 1995. Analysis of mud filtration properties using factorial design.

John, O., 2017. The effect of temperature on cement slurry using fluid loss additive. American Journal of Engineering Research (AJER), 6(8), pp.136-151.

Keller, S.R., Crook, R.J., Haut, R.C. and Kulakofsky, D.S., 1983. *Problems associated with deviated-wellbore cementing* (No. CONF-8310121-). Exxon Production Research Co..

Kutasov, I.M., 2002. Method corrects API bottomhole circulating-temperature correlations. *Oil & gas journal*, *100*(28), pp.47-47.

Labibzadeh, M., 2010. Assessment of the early age tensile strength of the oilfield class G cement under effects of the changes in down-hole pressure and temperature. Trends Appl. Sci. Res. 5 (3), 165-176. https://doi.org/10.3923/tasr.2010.165.176

Labibzadeh, M., Zahabizadeh, B. and Khajehdezfuly, A., 2010. Early-age compressive strength assessment of oil well class G cement due to borehole pressure and temperature changes. *Journal of American Science*, *6*(7), pp.38-47.

Lanka, S.T., Moses, N.G.A., Suppiah, R.R. and Maulianda, B.T., 2021. Physio-chemical interaction of Ethylene-Vinyl Acetate copolymer on bonding ability in the cementing material used for oil and gas well. *Petroleum Research*, *7*(3), pp.341-349.

Lei, X., Li, X., Yu, X., Zhang, Z.J., Qi, Z.G. and Hu, J., 2015. Research on method for evaluating self healing cement performance. *Advances in Fine Petrochemicals*.

Maeso, C. and Tribe, I., 2001, September. Hole shape from ultrasonic calipers and density while drilling-a tool for drillers. In *SPE Annual Technical Conference and Exhibition*. OnePetro.

Mansur, A.A., do Nascimento, O.L. and Mansur, H.S., 2009. Physico-chemical characterization of EVA-modified mortar and porcelain tiles interfaces. *Cement and Concrete Research*, *39*(12), pp.1199-1208.

Nelson, E., & Guillot, D. 2006. *Well Cementing* (2nd Edition). Schlumberger.

Ozyildirim, H.C., 2011. *Laboratory investigation of lightweight concrete properties* (No. FHWA/VCTIR 11-R17). Virginia. Dept. of Transportation.

Raheem, A.A., Soyingbe, A.A. and Emenike, A.J., 2013. Effect of curing methods on density and compressive strength of concrete. *International Journal of Applied Science and Technology*, *3*(4).

Recommended Practice for Testing Well Cements, July 2005. API Recommended Practice 10B-2. ISO 10426-2:2003.

Reinhardt, H.W. and Jooss, M., 2003. Permeability and self-healing of cracked concrete as a function of temperature and crack width. *Cement and concrete research*, *33*(7), pp.981-985.

Richhariya, G., Dora, D.T.K., Parmar, K.R., Pant, K.K., Singhal, N., Lal, K. and Kundu, P.P., 2020. Development of self-healing cement slurry through the incorporation of dual-encapsulated polyacrylamide for the prevention of water ingress in oil well. *Materials*, *13*(13), p.2921.

Rike, J.L., 1973, September. Obtaining Successful Squeeze-Cementing Results. In *Fall Meeting of the Society of Petroleum Engineers of AIME*. OnePetro.

Rupnow, T.D. and Icenogle, P., 2011. *Evaluation of surface resistivity measurements as an alternative to the rapid chloride permeability test for quality assurance and acceptance* (No. FHWA/LA. 11/479). Louisiana Transportation Research Center.

Satiyawira, B., Fathaddin, M.T. and Setiawan, R., 2010, April. Effects of lignosulfonate and temperature on compressive strength of cement. In *Proceedings of the World Geothermal Congress* (pp. 1-3).

Sauer, C. W., & Till, M. V. 1985. Mud Displacement During the Cementing Operation. *Society of Petroleum Engineers*.

Sauki, A. and Irawan, S., 2010. Effects of pressure and temperature on well cement degradation by supercritical CO2. *International Journal of Engineering & Technology IJET-IJENS*, *1*(04), pp.53-61.

Shahvali, A., Azin, R. and Zamani, A., 2014. Cement design for underground gas storage well completion. *Journal of Natural Gas Science and Engineering*, *18*, pp.149-154.

Sun, F., Lv, G. and Jin, J., 2006, December. Application and research of latex tenacity cement slurry system. In *International oil & gas conference and exhibition in China*. OnePetro.

Suman. G. 0. Jr. and Ellis, R. E.: World Oil's Cementingg Oil and Gas Wells Including Casing Handling Procedures, Books on Demand, Ann Arbor, MI (1977).

Thiercelin, M.J., Dargaud, B., Baret, J.F. and Rodriquez, W.J., 1998. Cement design based on cement mechanical response. *SPE drilling & completion*, *13*(04), pp.266-273.

Wang, R. and Wang, P.M., 2011. Action of redispersible vinyl acetate and versatate copolymer powder in cement mortar. *Construction and Building Materials*, *25*(11), pp.4210-4214.

Wang, R., Wang, P.M. and Yao, L.J., 2012. Effect of redispersible vinyl acetate and versatate copolymer powder on flexibility of cement mortar. *Construction and Building Materials*, *27*(1), pp.259-262.

Wang, Q.Z., Wu, L.Z., 2004. The flattened Brazilian disc specimen used for determining elastic modulus, tensile strength and fracture toughness of brittle rocks: experimental results. Int. J. Rock Mech. Min. Sci. 41 (Suppl. 1), 26-30 https://doi.org/10.1016/j.ijrmms.2004.03.015

Wang, Q.Z., Jia, X.M., Kou, S.Q., Zhang, Z.X., Lindqvist, P.A., 2004. The flattened Brazilian disc specimen used for determining elastic modulus, tensile strength and fracture toughness of brittle rocks: analytical and numerical results. Int. J. Rock Mech. Min. Sci. 41 (2), 245-253. https://doi.org/10.1016/S1365-1609(03)00093-5

Wooley, G.R., Giussani, A.R., Galate, J.W. and Wedelich, H.F., 1984, September. Cementing temperatures for deep-well production liners. In *SPE Annual Technical Conference and Exhibition*. OnePetro.

Xi, F., Qu, J., Lv, G., Tan, W. and Wang, C., 2010, June. Study of deep water cement experimental method and cement slurry. In *The Twentieth International Offshore and Polar Engineering Conference*. OnePetro.

Yang, Y., Yuan, B., Sun, Q., Tang, X. and Yingquan, X., 2015. Mechanical properties of EVA-modified cement for underground gas storage. *Journal of Natural Gas Science and Engineering*, *27*, pp.1846-1851.

Yao, X. and Hua, S., 2007, February. Design of novel composite agent for improving the toughness of oil-well cement sheath. In *International Symposium on Oilfield Chemistry*. OnePetro.

Yuan, B., Yang, Y., Wang, Y. and Zhang, K., 2017. Self-healing efficiency of EVA-modified cement for hydraulic fracturing wells. *Construction and Building Materials*, *146*, pp.563-570.

Zhang, Z., Huang, Z., Zhou, Y., Sheng, M. and Wu, B., 2022. Characteristic of Spiral Displacement Process in Primary Cementing of Vertical Well Washout. *SPE Journal*, pp.1-13.

Zhou, Y.J. and Jia, J.H., 2010. A new type cement slurry system for deep and high temperature wells. *EJGE*, *15*, pp.1989-1995.

Appendix A: Thesis Project Timeline

Research Activity	Starts Date	End Date
Sample Preparation and Cement Material Mixing	15.01.23	03.02.23
Cement Sample Curing	15.01.23	03.02.23
Bonding Efficiency Evaluation Test	05.02.23	12.02.23
Cement Microstructure Test	15.02.23	18.02.23
Results Analysis and Final Report	18.02.23	1.04.23

Appendix B: Project Milestone

Milestone and Date	Date	Cumulative Project Completion (%)
Completion of Sample Preparation and Cement Material Mixing	03.02.23	10
Completion of Sample Curing	03.02.23	30
Completion of Bonding efficiency Evaluation Test	12.02.23	60
Completion of Cement Microstructure Test	18.02.23	80
Completion of Results Analysis and Final Report	01.04.23	100